Physics – Uspekhi **55** (6) 557 – 581 (2012)

REVIEWS OF TOPICAL PROBLEMS

PACS numbers: **75.85.+t**, **85.70.–w**, **85.75.–d**

Magnetoelectric and multiferroic media*

A P Pyatakov, A K Zvezdin

DOI: 10.3367/UFNe.0182.201206b.0593

Contents

Abstract. The last decade has witnessed a significant growth of research into materials with coupled magnetic and electric properties. Reviewed here are the main types and mechanisms of magnetoelectric interactions and conditions of their origin. Special attention is given to potentially practical materials that display magnetoelectric properties at room temperature. Example applications of magnetoelectric materials and multiferroics in information and energy saving technologies are discussed.

1. Introduction

The last decade has witnessed a significant growth of interest into materials with coupled electric and magnetic properties [1–14]. The results of these studies dating back to the discovery of the first magnetoelectrics were discussed in early reviews and monographs [15–19]. Up to the beginning of the 21st century, magnetoelectrics and multiferroics had attracted the attention of a rather narrow circle of specialists because small magnetoelectric (ME) effects and the low temperatures at which they manifested themselves hampered their practical application. The recent burst of research activity in this area (Fig. 1) is due to the discovery of materials displaying ME properties in moderate magnetic fields at room temperature. Years of intensive studies have not been wasted: the first decade of this century, which began with the question: "why are there so few magnetic ferroelectrics?" [1], ended with the question: "why are there so many of them?" [14].

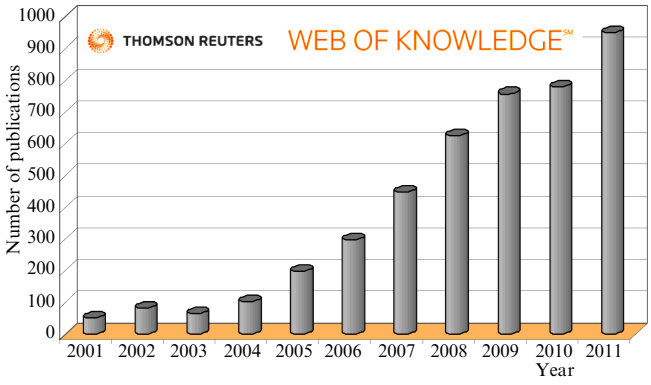

Figure 1. The number of publications on magnetoelectric materials and multiferroics in the first decade of the 21st century (taken from ISI Web of Knowledge).

The review outline is as follows. Section 2 familiarizes the reader with major ME phenomena. Section 3 deals with

A P Pyatakov Faculty of Physics, Lomonosov Moscow State University, Leninskie gory, 119991 Moscow, Russian Federation
Tel. +7 (495) 939 41 38. Tel./Fax +7 (495) 932 88 20
E-mail: pyatakov@physics.msu.ru
Prokhorov General Physics Institute, Russian Academy of Sciences, ul. Vavilova 38, 119991 Moscow, Russian Federation
A K Zvezdin Prokhorov General Physics Institute, Russian Academy of Sciences, ul. Vavilova 38, 119991 Moscow, Russian Federation
Tel. +7 (499) 503 83 35. Tel./Fax +7 (499) 135 02 47
E-mail: zvezdin@gmail.com

Received 6 February 2012
Uspekhi Fizicheskikh Nauk **182** (6) 593 – 620 (2012)
DOI: 10.3367/UFNr.0182.201206b.0593
Translated by Yu V Morozov; edited by A Radzig

* This review is an extended version of the report delivered at the scientific session of the Physical Sciences Division, Russian Academy of Sciences, dedicated to the 50th anniversary of RAS Scientific Council on Condensed Media Physics (9 November 2011) (see *Usp. Fiz. Nauk* **182** 559 (2012) [*Phys. Usp.* **55** 522 (2012)]). (*Editor's note.*)

materials most interesting for practical applications and displaying ME properties at room temperature, such as bismuth ferrite-based materials, iron garnet films, and their ilk. Finally, Section 4 considers potential applications of magnetoelectrics.

2. Magnetoelectric phenomena in magnetically ordered media

2.1 Linear magnetoelectric effect

Similar to electromagnetism as described by the Maxwell equations, the physics of magnetoelectric phenomena rapidly developing these days deals with the fundamental problem of the relationship between electric and magnetic phenomena. Despite a formal resemblance between the two notions, they concern effects of different natures. Electromagnetic phenomena are closely related to electrodynamics, i.e., they originate from the motion of electric charges or from variations of electric and magnetic fields in time. Magnetoelectric effects cannot be reduced to dynamic ones: even a static electric field induces magnetization, while a static magnetic field gives rise to electric polarization. As a matter of practice, this may be an important advantage allowing one to avoid thermal losses associated with flowing electric currents; hence, an intriguing possibility of designing magnets turned on and off by applying constant electric voltage rather than by conveying current. Such magnets, like permanent ones, would not require energy expenditure to maintain a magnetized state.

Pierre Curie [20] was the first to presume the existence of substances whose molecules are magnetized by the action of an electric field, and electrized by a magnetic field. His ideas were later developed by S A Boguslavskii [21], P Debye [22], and L Néel. B D H Tellegen designed a composite magnetoelectric medium in the form of suspended magnetized particles attached to electret pieces [23]. Nevertheless, no ME materials in the form of either composites or single-phase media were available up to the mid-20th century.

In 1956, L D Landau and E M Lifshitz [24] elaborated the notion of ME materials. Since that time, this term has denoted media whose symmetry implies the existence of a *linear magnetoelectric effect*, i.e., the emergence of electric polarization proportional to the magnetic field, and magnetization proportional to the electric field (inverse ME effect):

$$M_i = \frac{\alpha_{ij}}{4\pi} E_j \,, \tag{1a}$$

$$P_i = \frac{\alpha_{ji}}{4\pi} H_j \,, \tag{1b}$$

where **M** is the magnetization, **E** is the electric field, **P** is the polarization, **H** is the magnetic field, and α_{ij} is the tensor of the ME effect.

Note that formulas (1) relate vectors of various transformation properties with respect to space (P) and time (T) inversion operations, viz. the polar vectors **P** and **E** changing sign upon spatial inversion and remaining unaltered upon time inversion (i.e. P-odd, T-even), and the axial vectors **M** and **H** (T-odd, P-even). Thus, violation of P-parity and T-parity severally, with combined PT parity being conserved, was regarded as a necessary condition for a linear ME effect to be manifested in matter; it considerably narrowed the search scope. In 1959, I E Dzyaloshinskii predicted the occurrence of an ME effect in Cr_2O_3 [25]. A year later,

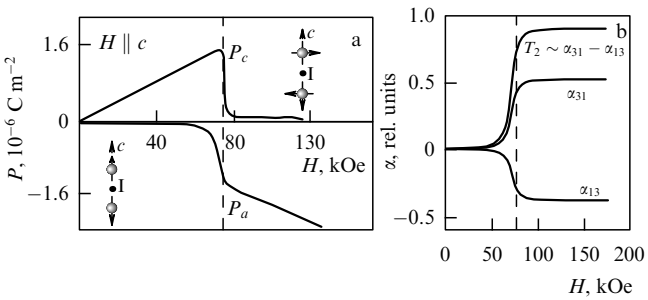

Figure 2. (a) Dependences of polarizations along the *a*- and *c*-axes on the magnetic field directed parallel to the *c*-axis of a Cr_2O_3 crystal [29]. The inset schematically shows an exchange structure with the center of symmetry I located between two magnetic Cr ions. (b) Nondiagonal components α_{13} and α_{31} of the tensor of the ME effect and the corresponding component of toroidal moment T_2. Dashed straight line separates two phase states: one with spins parallel to the *c*-axis (characterized by the longitudinal ME effect), and the other with spins normal to the *c*-axis (characterized by the transverse ME effect) [29].

D N Astrov observed magnetization (1a) induced by an electric field [26]. Soon after that, Folen, Rado, and Stalder [27] measured magnetic field-induced electric polarization (1b) in Cr_2O_3. In either case, the effect was a longitudinal one, i.e., induced polarization and magnetization vectors were parallel. Thereafter, it was shown that the ME effect in Cr_2O_3 becomes transverse in high magnetic fields due to the spin-flop phase transition [28, 29], in which spins initially directed along the principal *c*-axis 'flop' into the basal plane perpendicular to the *c*-axis.

The magnetic structure of Cr_2O_3 in both orientation states is illustrated in Fig. 2a. The magnetic ion exchange structure of this material is such that the inversion center transfers chromium ions from one antiferromagnetic sublattice to the other [25, 30]. Such a magnetic exchange structure is termed *centrally antisymmetric* [31]. Thus, the break of central symmetry in the magnetically ordered phase makes possible a linear ME effect. The orientation state determines the structure of the magnetoelectric tensor, so that its diagonal elements are nonzero in the easy-axis state, and nondiagonal ones are nonzero in the easy-plane state (longitudinal and transverse ME effects, respectively).

The transverse ME effect has recently attracted much attention in connection with the concept of the *toroidal or anapole moment* dual to the antisymmetric part of the ME effect tensor. The toroidal moment corresponding to one of the terms in the multipole expansion of vector potential $\mathbf{A}(\mathbf{r})$ is defined by the formula [32]

$$\mathbf{T} = \frac{1}{10c} \int \left[(\mathbf{jr})\mathbf{r} - 2r^2 \mathbf{j} \right] \mathrm{d}^3 r \,, \tag{2}$$

where **j** is the electric current density vector, **r** is the radius vector, and *c* is the speed of light. The simple geometric representation of the toroidal moment has the form of a toroidal solenoid.

Magnetic ordering that can be described by the toroidal moment vector is called *ferrotoroidal* [33–38]. In the case of Cr_2O_3, the ferrotoroidal phase is realized in high magnetic fields surpassing a spin-flop transition field of 80 kOe [39, 40]. Representation of magnetic ordering as localized magnetic moments makes it possible to rewrite formula (2) as

$$\mathbf{T} = \frac{1}{2} g\mu_\mathrm{B} \sum_i \mathbf{r}^i \times \mathbf{S}^i \,, \tag{3}$$

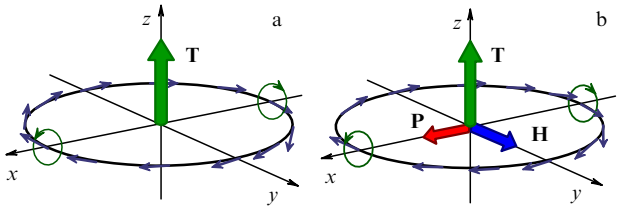

Figure 3. (a) Toroidal spin ordering. (b) Electric polarization **P**, besides magnetization, is induced in the external magnetic field.

where g is the ion Landé factor, μ_B is the Bohr magneton, $\mathbf{S}^i$ are spins, and $\mathbf{r}^i$ are the radius vectors of magnetic ions over which summation is carried out.

Note that formula (3) should be applied to solid-state physics problems with caution: its unrestricted use is feasible only in the case of size-limited specimens with zero magnetization. Otherwise, the toroidal moment will depend on the choice of the origin of coordinates with respect to which the moment described by formula (3) is counted. When considering a boundless periodic medium, a problem arises analogous to the one known long ago in the theory of ferroelectricity [41, 42]: the toroidal order parameter of such a medium should be defined, similar to polarization in ferroelectrics, as a change in the moment (3) arising under the action of alternating external factors or resulting from phase transition (see, for instance, Refs [43, 44]).

On the other hand, formulas (2), (3) are applicable unrestrictedly to magnetoelectric nanoparticles and mesoscopic objects, such as metal-organic clusters [45, 46]. These latter are of interest for the possibility of realizing the original idea of P Curie concerning ME molecules. We also note that a system possessing a toroidal moment has no stray field.

The diagram in Fig. 3 most demonstratively illustrates the relationship between the ME effect and toroidal moment. Let there be a system of ions with circularly ordered magnetic moments (Fig. 3a). The application of a magnetic field causes redistribution of magnetic moments and a rise in the number of ions with magnetic moments directed along the field vector. Spin density redistribution due to displacements of magnetic ions leads to charge density redistribution, giving rise to electric polarization (Fig. 3b). Vectors of polarization **P**, magnetization **M**, and toroidal moment **T** form a triad of mutually perpendicular vectors.

There are at least five types of units in which the linear ME effect is measured. The SI unit is [s m^{-1}]. The dimensionless quantity ($\alpha = 4\pi P/H$) is used in the CGS system, along with the off-system unit [C (m^2 Oe)$^{-1}$]. Technical units [V cm^{-1} Oe^{-1}] or [V A^{-1}] (1 V A^{-1} $\approx$ 0.8 V cm^{-1} Oe^{-1}) are frequently used in the literature; they can be converted into the former three if the permittivity of a given material is known [1 C (m^2 Oe)$^{-1}$ $= 0.01\varepsilon\varepsilon_0$ V cm^{-1} Oe^{-1}]. In addition, rationalized CGS units are used to measure the ME effect defined as $\alpha^{\mathrm{r}} = \alpha/(4\pi) = P/H$. Such a diversity of the units of measure leads to misunderstanding in literature devoted to this topic and erroneous estimates of ME effect magnitude. In what follows, the most common nonrationalized CGS units will be used.

The maximum magnitude of the ME effect in a classical chromite Cr_2O_3 magnetoelectric at 260 K amounts to $\alpha = 10^{-3}$ CGS (3.7 ps m^{-1} or 20 mV cm^{-1} Oe^{-1}). It is much greater ($\sim$ 300 ps m^{-1} or 10^{-1} in CGS) for $TbPO_4$ [47] and

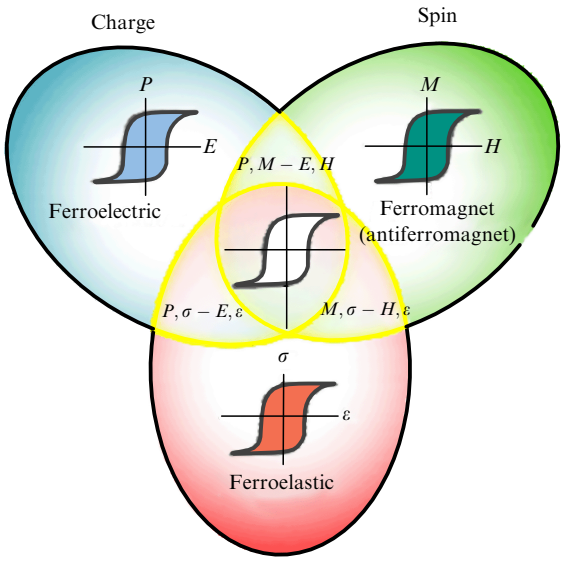

Figure 4. Three classes of 'ferroic' substances: ferroelectrics, ferromagnets (antiferromagnets), and ferroelastics. Each class displays characteristic hysteresis loops: $P(E)$, $M(H)$, $\sigma(\varepsilon)$, where σ and ε are mechanical stress and strain, respectively. Multiferroics lie at the intersections of these sets: $P, M-E, H$ is the region corresponding to ferroelectromagnets, $P, \sigma-E, \varepsilon$ — to ferroelectrics with ferroelastic properties, and $M, \sigma-H, \varepsilon$ — to materials with magnetic and ferroelastic orderings.

Ho_2BaNiO_5 [48]. It is generally agreed to describe such effects as 'giant'. However, the ME effect in the above materials occurs only at low temperatures.

High magnitudes of the ME effect at room temperature are obtained only in composite materials, i.e., in structures consisting of alternating magnetostrictive and piezoelectric layers [49–53]. Such a combined material behaves as effective magnetoelectric media in which ME interactions are mediated through a mechanical subsystem. Here, ME effects amount to 0.1 V cm^{-1} Oe^{-1} in a permanent magnetic field, and tens or hundreds of V cm^{-1} Oe^{-1} in an alternating magnetic field at an electromechanical resonance frequency, depending on the sample size and characteristics of the composite [49, 53].

2.2 Multiferroics and magnetoelectric phenomena in them

G A Smolenskii et al. [54] synthesized the very first $(1-x)Pb(Fe_{2/3}W_{1/3})O_3 - xPb(Mg_{1/2}W_{1/2})O_3$ *ferroelectromagnet*, i.e., a medium in which two types of ordering — magnetic and ferroelectric — coexist, at approximately the same time as the ME effect was discovered. Today, ferroelectromagnets are increasingly frequently named for the more general class of *multiferroics* (Fig. 4). The term multiferroic was coined by H Schmid [55] to denote matter in which at least two of the three types of ordering are simultaneously present, viz (1) ferromagnets (antiferromagnets), (2) ferroelectrics, and (3) ferroelastics. In what follows, we shall use the terms 'multiferroic' and 'ferroelectromagnet' equivalently, in line with established tradition.

Ferroelectric polarization and magnetic ordering co-exist only in matter with frustrated spatial and time inversion, which imposes serious limitations on the number of symmetry groups in multiferroics (e.g., the coexistence of magnetization and electric polarization is permitted only for 13 of the 122 Shubnikov point groups).

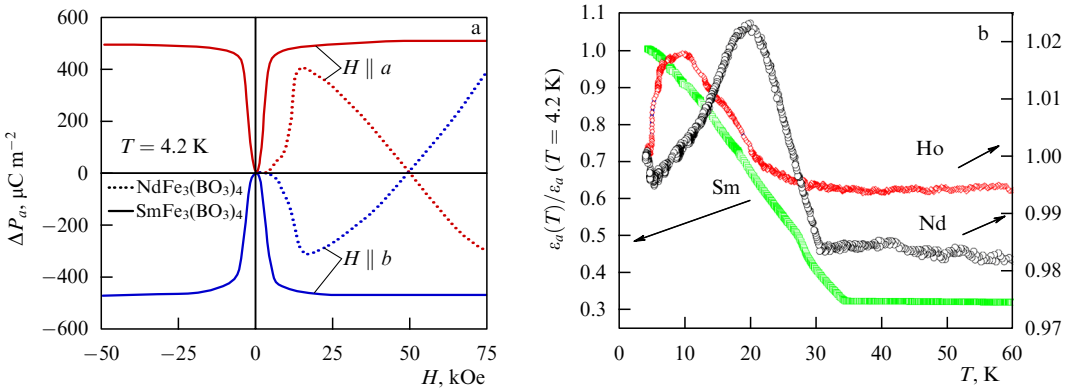

Figure 5. Magnetoelectric and magnetodielectric effects in rare-earth iron borates $R\mathrm{Fe}_3(\mathrm{BO}_3)_4$. (a) Appearance of electric polarization in samarium $\mathrm{SmFe}_3(\mathrm{BO}_3)_4$ (solid curve) and neodymium $\mathrm{NdFe}_3(\mathrm{BO}_3)_4$ (dotted curve) iron borates on establishing homogeneous antiferromagnetic ordering (magnetic field strength ~ 10 kOe), and polarization switching to the opposite sign upon a change in the direction of the antiferromagnetic vector from *a*-axis to *b*-axis of the crystal [56]. (b) Temperature dependences of permittivity (normalized to its value at $T = 4.2$ K) for Sm, Nd, and Ho iron borates [57].

Another circumstance making magnetic and ferroelectric ordering seemingly incompatible is the fundamental difference in electronic structure: in fact, the magnetic properties of atoms are determined by ions with partially occupied d-orbitals, whereas the electric dipole moment in ferroelectrics, as a rule, arises from stereochemical activity of a lone pair (2-valence s-electrons) [1]. However, this limitation does not apply to substances in which electric polarization is due to P-parity violation in the magnetic subsystem. In such ferroelectrics, electric polarization is not merely coexistent with magnetic ordering but originates from it, while the temperature of ferroelectric ordering is either below or equal to the magnetic ordering temperature. Ferroelectrics with magneto-induced polarization are also known as *type* 2 *multiferroics* [11], to be distinguished from their *type* 1 historical predecessors whose ferroelectric ordering temperature is higher than the magnetic ordering temperature (e.g., one of the first synthesized ferroelectromagnet BiFeO_3 [15]).

The coexistence of magnetic and ferroelectric subsystems implies interaction between them. Media with magnetic and electric ordering can be expected to exhibit higher-order nonlinear electric and magnetic field effects (quadratic and cubic), besides a linear one, as well as switching of electric polarization controlled by a magnetic field (see, for instance, Refs [56, 57]) (Fig. 5a), and of magnetization by an electric field [58]. Moreover, ME effects can manifest themselves as electric field-induced magnetic phase transitions [58] and inverse effects [59].

Such ME interactions are described by contributions to the thermodynamic potential, i.e., invariant combinations including magnetic order parameter **M** or antiferromagnetic vector **L** and electric polarization **P**.

The most obvious combination satisfying the P- and T-parity condition and invariance with respect to symmetry elements (rotation axes and mirror planes) is the P^2M^2 type biquadratic contribution [15].

This universal interaction must be present in any multiferroic where it causes a temperature shift of magnetic or ferroelectric ordering and thereby leads to renormalization of susceptibility values. However, it cannot promote, for example, magnetically induced polarization. It is only the contribution linear in the secondary order parameter (e.g., polarization) that can lead to magnetically induced polarization and associated strong magnetoelectric effects. Interactions of this type are naturally realized in crystals lacking an inversion center, as well as in piezoelectric [60] and nonpolar media without a symmetry center in the form of magneto-induced polarization. A good example of nonpolar media without the symmetry center is a new class of multiferroics — rare-earth iron borates [61–69] [general formula $R\mathrm{Fe}_3(\mathrm{BO}_3)_4$], where R is a rare-earth element. Such media — extensively studied in recent years — display ferroelectric properties at temperatures lower than antiferromagnetic ordering temperature T_N.

It would seem that a combination like PM^2 is forbidden in a centrosymmetric crystal. However, the situation is not as simple as that in magnetically ordered matter with a few sublattices. Specifically, the invariant can be written in the form of the sum over different magnetic sublattices (s and s′):

$$f_\mathrm{ME}^\mathrm{lin} = -\frac{1}{2}\sum_{ss'} \gamma_{ss'}^{ijk} P^i M_s^j M_{s'}^k \,. \tag{4}$$

The invariant may include antiferromagnetic order parameters. The simplest example is an antiferromagnet with two magnetic sublattices, characterized by the order parameter $\mathbf{L} = \mathbf{M}_1 - \mathbf{M}_2$. In the above case of $\mathrm{Cr}_2\mathrm{O}_3$ chromite (see Fig. 2), the symmetry center of a crystallochemical cell links magnetic ions of different antiferromagnetic sublattices, while vector **L** can be both P- and T-odd; in other words, invariants may have the forms

$$f_\mathrm{ME}^\mathrm{lin1} \sim E_i H_j L_k \,, \tag{5}$$

$$f_\mathrm{ME}^\mathrm{lin2} \sim P_i M_j L_k \,. \tag{6}$$

Invariant (5) corresponds to the linear ME effect considered in preceding paragraphs, and invariant (6) describes the relationship between spontaneous magnetization, the antiferromagnetic vector, and ferroelectric polarization in multiferroics.

As the number of magnetic sublattices increases, the inversion operation can transform one antiferromagnetic mode, L_1, to another, L_2; hence, the possibility of composing P-odd combinations of antiferromagnetic modes, and expression (4) takes the form

$$f_\mathrm{ME}^\mathrm{lin3} \sim P(L_1^2 - L_2^2) \,. \tag{7}$$

In this way, the emergence of electric polarization in $R\mathrm{Mn_2O_5}$ manganites [70–72], $\mathrm{LiCu_2O_2}$ cuprates [73–75], and other substances is explained.

An additional characteristic property of multiferroics is the *magnetodielectric effect* (or *magnetocapacity*), i.e., the dependence of dielectric constant on the magnetic field [76]. Relative changes in dielectric constant under exposure to a magnetic field as high as ~ 1 T amount to tens and hundreds of percent in orthorhombic rare-earth $R\mathrm{MnO_3}$ (R = Eu, Gd, Tb, Dy) manganites [77] and rare-earth $R\mathrm{Fe_3(BO_3)_4}$ iron borates [78]. Also, the magnetodielectric effect is manifested as a change in dielectric constant upon the establishment of magnetic ordering and the emergence of ferroelectric polarization in type 2 multiferroics (Fig. 5b).

The ME phenomena described above occur in static electric and magnetic fields; moreover, they can be observed within a high-frequency range [79, 80]. The discovery of a new type of elementary excitations — *electromagnons* [81, 82], which unlike magnons, respond to the electric rather than magnetic component of an electromagnetic wave, suggests new nontrivial effects at high frequencies, because the magnitude of dynamic ME effects underlain by isotropic Heisenberg exchange may even surpass that of static effects caused by spin-orbit interaction [83]. Theoretical work [84] predicts the possibility of electric polarization switching on picosecond time scales by terahertz radiation pulses.

Magnetoelectric and ferroelectric properties can also manifest themselves in the magneto-optical properties of materials. For example, linear and quadratic ME effects are exhibited as variations of the angle of light polarization rotation in the Faraday effect (electromagneto-optical effect) [85–88] (see Section 4.4) or the dependence of the absorption coefficient on the relative orientation of the wave vector and toroidal moment [89, 90].

Central symmetry breaking in a crystal undergoing magnetic ordering is a necessary condition for the existence of a linear ME effect and magnetically induced electric polarization in type 2 multiferroics; it is also responsible for the generation of the second optical harmonic induced in response to magnetic ordering [91–95]. This phenomenon was first observed in $\mathrm{BiFeO_3}$ bismuth ferrite, a type 1 multiferroic [91]; specifically, the contribution from the magnetic ordering arising for $T < T_\mathrm{N}$ increased as $I_{2\omega} \sim (T - T_\mathrm{N})^2$ to reach values a few orders of magnitude higher than the contribution due to electric polarization (Fig. 6). Such temperature dependence can be accounted for by the proportionality of the nonlinear magneto-optical response characterized by polarization $P_{2\omega}$ to the square of the antiferromagnetic order parameter: $P_{2\omega} \sim L^2$ [96]. The method of generation of the second harmonic has proved itself to be a powerful tool for the study of magnetoelectrics and multiferroics [97–102], allowing visualization of ferroelectric [2, 103], magnetoelectric [104], and ferrotoroidal [105] domains.

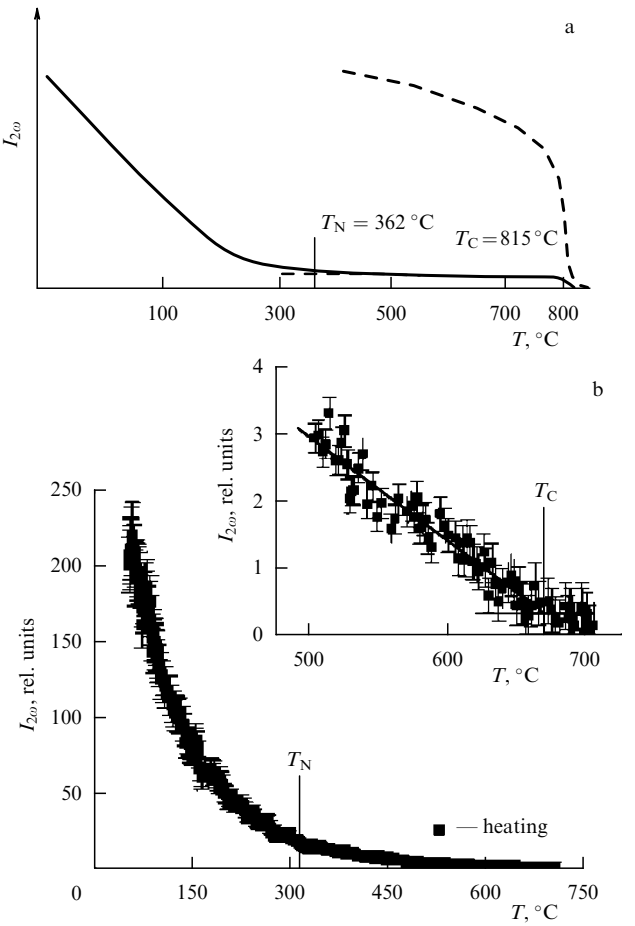

Figure 6. (a) Temperature dependence of second optical harmonic intensity $I_{2\omega}$ in bismuth ferrite $\mathrm{BiFeO_3}$ (solid curve); T_N and T_C are temperatures of magnetic and ferroelectric orderings, respectively [91]. The dashed curve shows second harmonic intensity for $T < T_\mathrm{C}$ (10-fold magnification). (b) Temperature dependence for bismuth ferrite films. The inset depicts second harmonic intensity (magnified) near the Curie point: temperature of ferroelectric ordering drops dramatically due to the creation of mechanical stresses inside the films (reproduced with generous permission of T V Murzina [94]).

2.3 Multiferroics with spatially modulated spin structures. Spin-flexoelectric effect

The large group of multiferroics comprises media characterized by nonuniform distribution of the magnetic order parameter. The spatial modulation period of sublattice magnetization in these substances may be a few orders of magnitude greater than the unit cell size. Inhomogeneous ME interactions also occurring in them [15, 106] are described by invariant combinations linear in electric polarization and having the form $P_i M_j \nabla_k M_l$. Inhomogeneous ME interactions are manifested as spatially modulated spin structures induced by electric polarization or as an inverse effect, i.e., electric polarization induced by such structures. The latter scenario of the emergence of ferroelectricity is so common among multiferroics that they tend to be divided into two classes by the type of prevailing ME interactions (homogeneous or inhomogeneous) rather than based on the origin of electric polarization [107].

In terms of symmetry, inhomogeneous ME effects are similar to *flexoelectric* (from Latin *flexus* — bent) phenomena in crystals, consisting in the emergence of electric polarization brought about by the deformation gradient [41, 107–111].

Indeed, examination of a crystal with the symmetry center exposed to an external mechanical impact reveals inversion symmetry breaking only in the case of bending, while the polar direction along the mechanical stress gradient is distinguished in accordance with the Curie principle, thus creating the necessary condition for the appearance of electric polarization (Fig. 7a–d).

In magnetically ordered media, the same result is achieved in the presence of the spin cycloid (Fig. 7e) which, unlike the helicoid (torsional strain analog) (Fig. 7f), specifies the polar direction in the crystal.

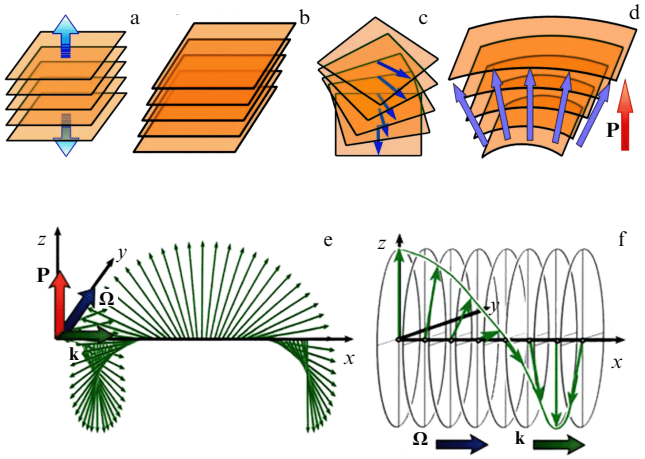

Figure 7. Different types of mechanical strain are as follows: (a) longitudinal, (b) shearing, (c) torsional, (d) bending. Only the last one distinguishes the polar direction in matter. Spatially modulated structures in magnetic media: (e) spin cycloid, and (f) spin helicoid.

In the case of cubic symmetry, the invariant corresponding to inhomogeneous magnetoelectric (flexomagnetoelectric) interaction assumes the simple form

$$F_{\mathrm{ME}}^{\mathrm{inh}} = \gamma\left[\mathbf{P}(\mathbf{m}\,\mathrm{div}\,\mathbf{m} + \mathbf{m}\times\mathrm{rot}\,\mathbf{m})\right], \tag{8a}$$

where γ is the coefficient characterizing inhomogeneous magnetoelectric (flexomagnetoelectric) interaction. For the common case of symmetry with the higher-order axis and the basal plane perpendicular to it (tetragonal and hexagonal syngony), the flexomagnetoelectric energy is written as

$$F_{\mathrm{ME}}^{\mathrm{inh}} = \gamma P_z\left(m_z(\nabla\mathbf{m}) - (\mathbf{m}\nabla)\,m_z\right), \tag{8b}$$

where the z-axis is parallel to the principal axis.

Having used representation (8b) and expressing the magnetization unit vector in spherical coordinates, $\mathbf{m} = (\sin\theta\cos\varphi, \sin\theta\sin\varphi, \cos\theta)$, we obtain $F_{\mathrm{ME}} = \gamma P_z\,\partial\theta/\partial\xi$, where ξ is the coordinate along the modulation direction or $F_{\mathrm{ME}} = \gamma\mathbf{P}[\mathbf{k}\times\boldsymbol{\Omega}]$ in terms of the wave vector $\mathbf{k}$ of spatially modulated spin structure and the normal $\boldsymbol{\Omega}$ to the plane of magnetization rotation. Electric polarization in spatially modulated structures is represented as the vector product of $\mathbf{k}$ and $\boldsymbol{\Omega}$ [112]:

$$\mathbf{P} = -\frac{\partial F_{\mathrm{ME}}}{\partial\mathbf{E}} = \gamma\chi_{\mathrm{e}}\mathbf{k}\times\boldsymbol{\Omega}, \tag{9}$$

where χ_{e} is the electric polarizability. This implies zero electric polarization for the spin helicoid (Fig 7f). Furthermore, it follows from formula (9) that polarization is highest for the spin cycloid, while a change in the direction of magnetization rotation in the cycloid, $\boldsymbol{\Omega}\to-\boldsymbol{\Omega}$, results in polarization switchover: $\mathbf{P}\to-\mathbf{P}$.

This mechanism of polarization emergence, frequently called 'spiral' in the literature [112], proved to be a very convenient model for explaining and predicting ME phenomena associated with incommensurate magnetic structures [113]. Also, a plausible explanation was given to polarization jumps in $BiFeO_3$ [114] (Fig. 8a) and $BaMnF_4$ [10] compounds, and to the effects observed in orthorhombic $R\mathrm{MnO_3}$ manganites, such as electric polarization rotation by 90° under the action of a magnetic field turning over the helical plane (Fig. 8b) [115, 116], and the switchover effect of the spin-cycloid rotation direction (vector chirality) under the action of the electric field [117, 118] (Fig. 8c).

The above narrow class of multiferroics is not the sole one in which the spin-flexomagnetoelectric mechanism of electric polarization is inherent. Long before it was 'rediscovered', the relationship between spatially modulated spin structures and electric polarization in orthorhombic manganites had been postulated when considering the causes of ferroelectric ordering in Cr_2BeO_4 [15, 119] and presenting the spin cycloid in $BiFeO_3$ [120]. A few dozen new spiral multiferroics were described in the 2000s; special review articles were devoted to these materials [10, 121, 122].

In the majority of these compounds, ME effects associated with the formation, destruction, transformation, and reorientation of the spin-cycloid plane (see Fig. 8) occur at low temperatures and high magnetic fields (several or tens of teslas). However, a few recent publications suggest the possibility of such effects in weak magnetic fields (several mT or tens of mT) in the hexaferrite $Ba_2Mg_2Fe_{12}O_{22}$ [123], and at room temperature in $Sr_3Co_2Fe_{24}O_{41}$ [124, 125].

The redeeming simplicity of the explanation of ME phenomena in spiral multiferroics and their widespread occurrence has led some researchers to believe in the universal character of the spin-flexoelectric mechanism of ferroelectricity as some sort of magnetoelectric paradigm. However, the switching over of spin rotation direction $\boldsymbol{\Omega}$ in many type 2 multiferroics (orthorhombic $R\mathrm{Mn_2O_5}$ manganites, $R\mathrm{Fe_3(BO_3)_4}$ iron borates, $LiCu_2O_2$ cuprates, etc.) does not change the sign of electric polarization and polarization arises in the commensurate magnetic structure or magnetic moments are collinear. Moreover, electric polarization appearing together with the spin helicoid in the delafossites $CuFe_{1-x}Al_xO_2$, $CuCrO_2$ [126–128] and in $CaMn_2O_7$ compound [129] is directed along its axis, which cannot be

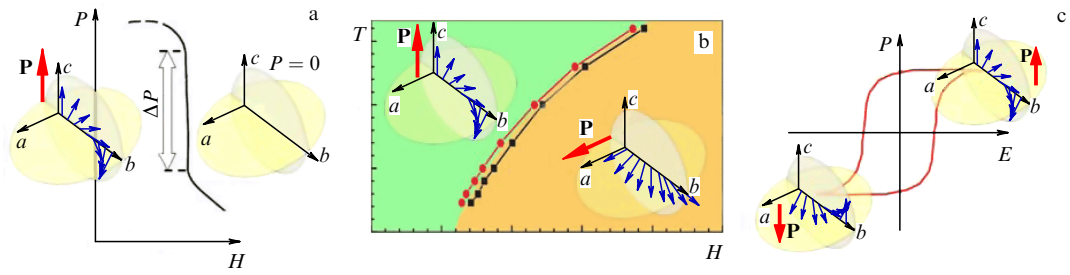

Figure 8. ME effects associated with spin cycloids: (a) polarization jumps upon cycloid suppression (formation), (b) a change in the cycloid plane during spin-reorientation transition, and (c) a change in the cycloid rotation direction upon electric polarization switchover.

accounted for by the spin-flexoelectric mechanism obeying rule (9). Original crystal symmetry in the above cases is devoid of the second-order symmetry axis in the direction normal to the helicoid wave vector [126], whereas formulas (8), (9) were derived for isotropic and high-symmetry cases.

2.4 Microscopic mechanisms of magnetically induced electric polarization

The authors of early studies initiated soon after the discovery of a linear ME effect suggested two main (single- and two-ion) microscopic mechanisms of its development [130]. The former implies the dependence of spin Hamiltonian parameters of a magnetic ion (primarily its g-factor) on the electric field [131] (see also the article by G T Rado in Ref. [18, p. 3]). Such dependence results from the combined action of crystal field components that are odd with respect to spatial inversion, spin–orbit interaction, and interaction with external electric and magnetic fields. The two-ion mechanism is based on the dependence of exchange interactions (isotropic Heisenberg [132] and asymmetric [133] ones) on the coordinates of magnetic ions and intermediate ligands, e.g., oxygen. The single-ion mechanism is usually realized in rare-earth materials, while the two-ion one predominates in materials whose magnetic properties depend on d-ions (Fe, Ni, Co, Mn, etc.). Reference [130] overviews publications dealing with these mechanisms.

Mechanisms related to Dzyaloshinskii–Moriya antisymmetric exchange ($\mathbf{D}[\mathbf{S}_1 \times \mathbf{S}_2]$) (Fig. 9a) [7, 121] have recently been attracting a good deal of attention. They became topical in connection with investigations into novel ME materials of incommensurate magnetic structure [134], where the direction of ion magnetic moment varies from one point to another with a period that is not a multiple of the crystal lattice period and, as a rule, is much larger than that (Fig. 9b). A displacement of a ligand ion in accordance with the known Keffer formula $\mathbf{D} \sim \mathbf{r}_1 \times \mathbf{r}_2$ [135, 136], where $\mathbf{r}_1$ and $\mathbf{r}_2$ are the radius vectors directed from the ligand ion to magnetic ions, causes a change in the Dzyaloshinskii vector and, therefore, a canting of antiferromagnetic sublattices (Fig. 9a). The inverse effect is equally possible, i.e. induction of polarization by a magnetic field. The Dzyaloshinskii–Moriya antisymmetric exchange is responsible for the coupling of spin cycloids and electric polarization in spiral multiferroics (Fig. 9b).

Spin rotation is unnecessary for ME interactions caused by symmetric Heisenberg exchange, which are described by the scalar product of interacting ion spins, $\mathbf{S}_1\mathbf{S}_2$. Electric polarization through a nonrelativistic (exchange striction) mechanism [137] can occur even in collinear structures (Fig. 9c), which does not exclude its presence in materials with noncollinear or commensurate spatially modulated spin structures due to the usual dominance of the nonrelativistic contribution [73].

It should be noted that under both (relativistic and nonrelativistic) mechanisms, electric polarization can be induced by ion displacement in the crystal lattice (see Fig. 9) as well as by electron density redistribution [73]. Generation of the second optical harmonic, suggesting a substantial electron contribution to electric polarization, allows observing ferroelectric domains formed by spin cycloids with opposite chiralities [100].

The development of other observational methods allowing the researcher to distinguish between electron and ion contributions to polarization is also currently underway. One of them, proposed in Ref. [138], makes it possible to detect ion displacements on scales from tens of to a few femtometers in orthorhombic $TbMnO_3$ manganites of a family of spiral multiferroics. The measurements were based on the interference between two contributions: the 'charge' contribution resulting from X-ray diffraction by the crystal lattice, and the 'magnetic' contribution resulting from ray scattering on the spin cycloid. Estimates of ion displacement due to spontaneous electric polarization, ranging (20 ± 3) fm, suggest the ionic mechanism of ferroelectricity in the given class of multiferroics.

2.5 Magnetoelectric properties of interfaces

A surface forming a common boundary between adjacent media, namely interface may have properties that are absent in either bulky material. In this context, it is worth noting symmetry breaking with respect to space/time inversion at the boundary between dielectric and magnetic media or at the magnet–insulator interface; specifically, there is no symmetry center in the near-surface layers at the interface, while magnetic ordering in one of the media breaks time reversal symmetry. Thus, prerequisites for an ME effect are created at the interface.

Herbert Kroemer said in his 2000 Nobel lecture: "The interface is the device." A spin capacitor concept in the spirit of this maxim was proposed according to which spin-polarized electrons accumulate at the magnetic metal–insulator interface under the action of an electric field [139, 140]. Such a device for the realization of ME effects is structurally similar to composite materials, the main difference being that its magnetic and electric subsystems are not spatially separated but co-exist, even if within a very thin layer. Electric polarization spreads through the magnetic material as deep as a few atomic layers and thus turns it to magnetoelectric one.

For a similar reason, a diamagnetic ferroelectric material may display properties inherent in multiferroics at the boundary of a magnetic medium (Fig. 10a, b). Such a phenomenon was predicted in Ref. [141] and confirmed in experiments on the $BaTiO_3/Fe$ [142] and $BaTiO_3/Co$ [140] structures: circularly polarized X-ray scattering spectra from Ti^{4+} ions gave evidence that magnetic order ranges

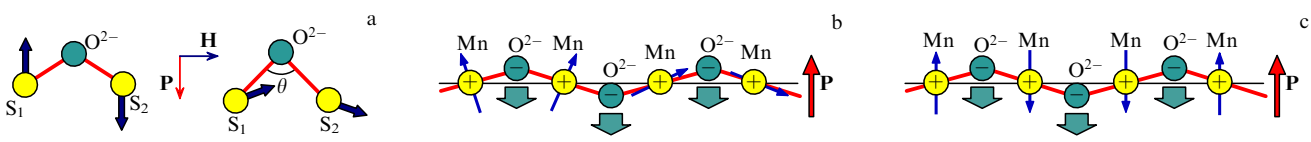

Figure 9. Mechanisms of the ME effect and magneto-induced electric polarization in multiferroics: (a) polar ion displacements altering the angle between magnetic ion–ligand bonds and affecting the relative orientation of magnetic moments [44]; (b) coupling between spatial spin modulation and electric polarization underlain by the relativistic mechanism [134], and (c) changes in bond angles and polar ion displacements via the nonrelativistic mechanism [137].

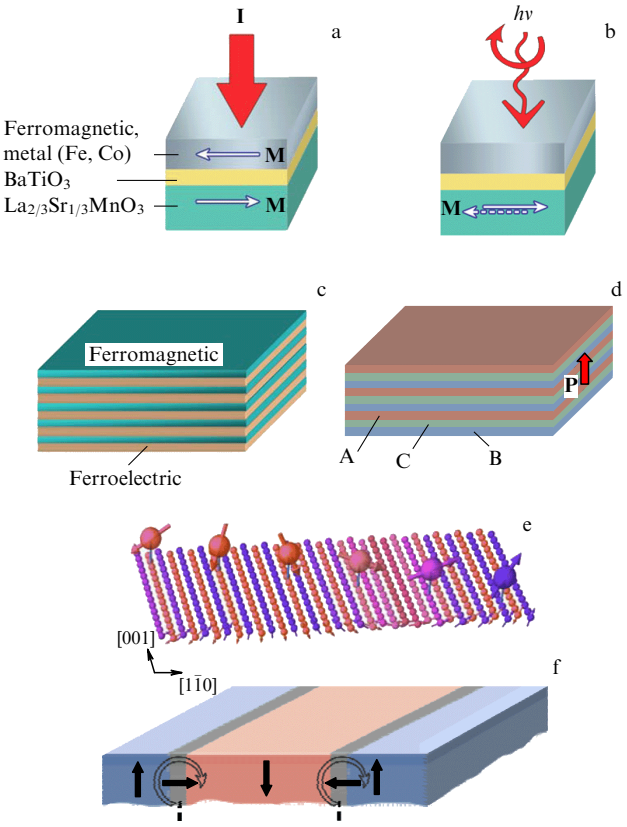

Figure 10. Magnetoelectric properties of surfaces and interfaces: (a, b) a structure containing a nanometer-sized barium titanate (BTO) layer between iron (cobalt) electrodes and an $La_{2/3}Sr_{1/3}MnO_3$ (LSMO) layer; resistance of the structure depends on the polarization direction in BTO and the mutual magnetization (**M**) direction in the electrodes [140]; scattering spectra from Ti ions depend on the X-ray circular polarization direction [140]. Magnetic superlattices with multiferroic properties: (c) alternating ferromagnetic and ferroelectric layers, and (d) three-component multilayered structure. (e) Cobalt atoms deposited onto the Mn monolayer surface at equal distances from one another: arrows indicate spins of Co and Mn atoms in the layer. (f) Schematic representation of micromagnetic distribution in iron garnet films.

across the $BaTiO_3$ ferroelectric over a few lattice periods [140].

Current investigations involve not only ordinary insulators but also so-called topological insulators [143–145] having no band gap for surface states. Coating a topological insulator with a magnetic film, adding magnetic impurities, or placing it in a magnetic field results in breaking time inversion and lead, in turn, to the formation of a band gap and occurrence of a strong ME effect defined by the fine-structure constant $\alpha = 1/137$ [145]. Such an ME interaction was formerly considered in the physics of elementary particles in connection with the elucidation of the electrodynamic properties of a hypothetical axion particle [146].

Phenomena developing at interfaces just as well create additional possibilities in composite systems with a characteristic layer size of several interatomic distances. In such cases, the phases of composite materials influence each other's internal structure and properties, and ME properties manifest themselves not only at the boundaries but also in the bulk; as a result, the multilayer (ferroelectric/ferromagnetic) structure turns into an efficacious multiferroic (Fig. 10c) [147]. Finally, it is not necessary to use ferroelectric layers to break the central symmetry, needed for ME effects to show their worth; it will suffice to create a superlattice comprising three different magnetic components [148–150]: the layers alternating in one and the same order distinguish a polar direction A → B → C (Fig. 10d).

Reduction of symmetry at the interface also leads to the appearance of inhomogeneous ME effects. The author of Ref. [151] predicted the formation of the spin cycloid in ultrathin ferro- and antiferromagnetically ordered films. It was subsequently confirmed in experiments on magnetic ordering observation in manganese monolayers by scanning tunneling microscopy of spin-polarized electrons [152]. Measurements with the use of probes having different magnetic moment orientations revealed that the magnetic structure was the spin cycloid. The cycloid period (roughly 0.5 nm) was not much greater than the lattice period, with the angle between the spins of adjacent Mn atoms being 173°. In other words, an incommensurate spin structure was realized in the monolayer of ferromagnetic material (Fig. 10e). Such a cycloid may serve as a calibration grid to measure the image size and the probe magnetic moment, and as a sort of 'mounting plate': due to exchange interaction, atoms placed on its surface acquire a definite spin orientation, depending on their localization [153].

A domain structure formed instead of the magnetic cycloid in the double iron atomic layer epitaxially grown on a tungsten substrate with crystallographic orientation (110). Central symmetry breaking resulted in magnetization rotation within the domain boundaries that turned to be consistent with the Néel type domain wall [154]; in other words, the plane of such rotation became perpendicular to the domain boundary plane, with the direction of magnetization rotation being identical at all boundaries. Such a structure can be treated as a strongly distorted (soliton-like) spin cycloid. A similar phenomenon was observed in much thicker (≈ 10 μm) iron garnet films due to symmetry breaking as a result of the film growth [155] (Fig. 10f).

2.6 Domain boundaries

Domain walls represent a sort of interfaces with properties different from those of the medium in domains that they separate (see review [156] of domain wall electronics). Here are a few characteristic examples.

• *Electric polarization of domain boundaries.* Domain walls may be regarded as fragments of magnetic spirals. The same spin-flexoelectricity ideology as for 'spiral' multiferroics is applicable to them, a direct consequence being electric polarization of domain boundaries and the possibility of controling them by applying an electric field [106, 109], as shown experimentally in Refs [157, 158] (Fig. 11a).

• *The influence of the ferroelectric domain structure on the micromagnetic distribution in multiferroics.* Ferroelectric domain boundaries and magnetic domain boundaries in multiferroics proved to be coupled [2]. One of the feasible mechanisms underlying such coupling in multiferroics is the flexomagnetoelectric effect. A jump in electric polarization at the boundaries of ferroelectric domains must lead to a jump in spatial derivative of the magnetic order parameter [159], manifested as inhomogeneities in the magnetic structure at the boundaries (Fig. 11b). If magnetic (antiferromagnetic) and ferroelectric domain structures coexist in a given material, this effect can manifest itself as the *pinning* of magnetic domain boundaries at the boundaries of ferroelectric domains [160, 161]. It can be accounted for by the formation of a potential well for the magnetic

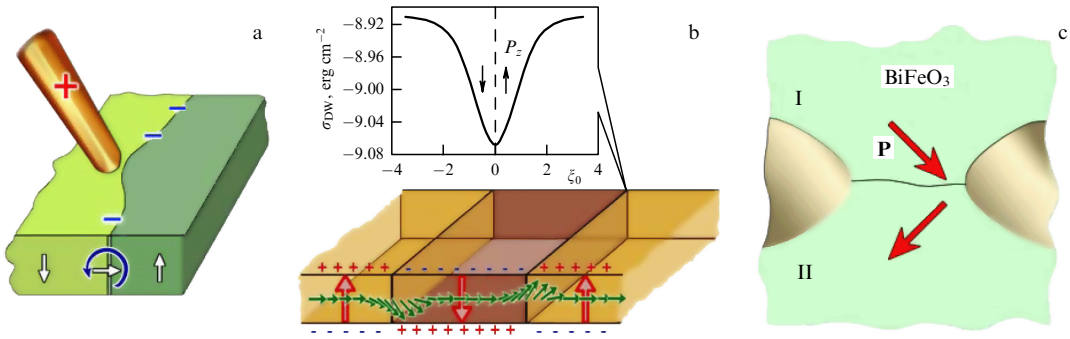

Figure 11. Properties of domain boundaries absent in the bulk of the domains. (a) Electric polarization of magnetic domain boundaries manifested in electrostatic interaction with a charged probe (attraction or repulsion depending on probe polarity). (b) The influence of ferroelectric domain boundaries on the micromagnetic and antiferromagnetic structure. The inset shows the dependence of the surface energy of magnetic domain boundaries on the distance to the ferroelectric domain boundary normalized to domain wall thickness [160]. (c) Domain boundaries as conducting channels whose number and location are controlled by the electric field [164, 166] (I and II mark the ferroelectric domains).

domain boundary near the ferroelectric domain boundary as a result of flexomagnetoelectric interaction (see the inset to Fig. 11b).

Recent theoretical work suggested the possibility of emerging magnetization at the sites of localization of ferroelectric domain boundaries even in antiferromagnetic substances [162, 163].

• *The emergence of local electric conductivity in ferroelectric domain boundaries*. This phenomenon was discovered when scanning the surface of a ferroelectric bismuth ferrite ($BiFeO_3$) with the use of a probe microscope in the resistive mode [164]. The resistivity of the domain boundary was only 1–10 Ω m or 5–6 orders of magnitude lower than that of the dielectric surroundings. Two possible causes were thought to be responsible for the enhanced conductivity in the domain boundary region: (1) the appearance of a potential barrier near the boundary, and the resulting rise in the concentration of charge carriers at this site (excess electric polarization of the domain boundary $\Delta P \sim 10$ mC cm^{-2} accounting for some 10% of the polarization in the domains), and (2) a narrowing of the band gap in a $BiFeO_3$ semiconductor by 3% (roughly 0.1 eV). Recent studies have shown that conductivity of domain boundaries varies — it can be 'switched over' (altered by more than one order of magnitude) by applying an electric field, thus making possible the design of memristors [165] (Fig. 11c).

We have considered different situations in which spatial inversion and time reversal are simultaneously violated, it being an intrinsic property of ME materials and multiferroics. We distinguish three main cases.

(1) Magnetic media whose group symmetry has no symmetry center; this may be either a property of the material belonging to the family of polar materials or due to magnetic ordering (ferroelectromagnets with a ferroelectric ordering of magnetic origin).

(2) Magnetic media with a broken symmetry center due to spatial modulation of the magnetic order parameter. The reduction of symmetry may be either local (micromagnetic structures like domain boundaries) or affect the entire crystal volume (spiral magnets).

(3) Surfaces and interfaces of dielectric and magnetic media, whose presence also causes a break of the symmetry center and thereby creates prerequisites for the emergence of ME phenomena at the boundaries.

The latter two cases substantially extend the range of materials exhibiting ME effects to include the media that retain central symmetry in a homogeneous magnetic state.

Practical applications of such materials may also be hampered by circumstances other than symmetry-related limitations, e.g., most magnetoelectrics and multiferroics exhibit their characteristic properties at low temperatures. Therefore, special attention is given to media with a magnetic ordering temperature above room temperature. Such magnetoelectrics are exemplified by Cr_2O_3 chromite (the first one discovered), and $BiFeO_3$-based multiferroics (see Section 3.1).

3. High-temperature multiferroics and magnetoelectric materials with promising applications

3.1 Perovskite-like multiferroics. Bismuth ferrite

Many magnetic insulators undergo crystallization into perovskite-like structures, such as $RFeO_3$ orthoferrites, $RMnO_3$ perovskite manganites, and $BiFeO_3$, $FeTiO_3$, and $BiMnO_3$ multiferroics. In the perovskite ABO_3, A-ions are localized at the sites of the cubic lattice surrounded by six oxygen ions in an octahedral arrangement. Such a structure forms at a certain ratio of the ion radii (the so-called geometric criterion) [167].

We shall consider the properties of multiferroics-perovskites exemplified by the best-known bismuth ferrite ($BiFeO_3$). This compound and those based on it are the subject of interest in almost one third of the studies on multiferroic properties. Synthesized in 1957 [168], bismuth ferrite is characterized by high-temperature electric ($T_C = 1083$ K) [169] and magnetic ($T_N = 643$ K) [170] ordering, a simple crystalline structure, and a variety of other properties (with practically all the types of ME interactions considered in Section 2 being realized in this material). As a result, bismuth ferrite has become a model object in magnetoelectric research discussed in special reviews [4, 171–175]. It is expected to have promising important applications in various fields, from spin electronics [166, 173, 174–179] and photonics [180–182] to medicine [183].

A unit cell in the $BiFeO_3$ perovskite phase [symmetry group $Pm3m$ (O_h^1)] is a cube with an Fe ion in the center

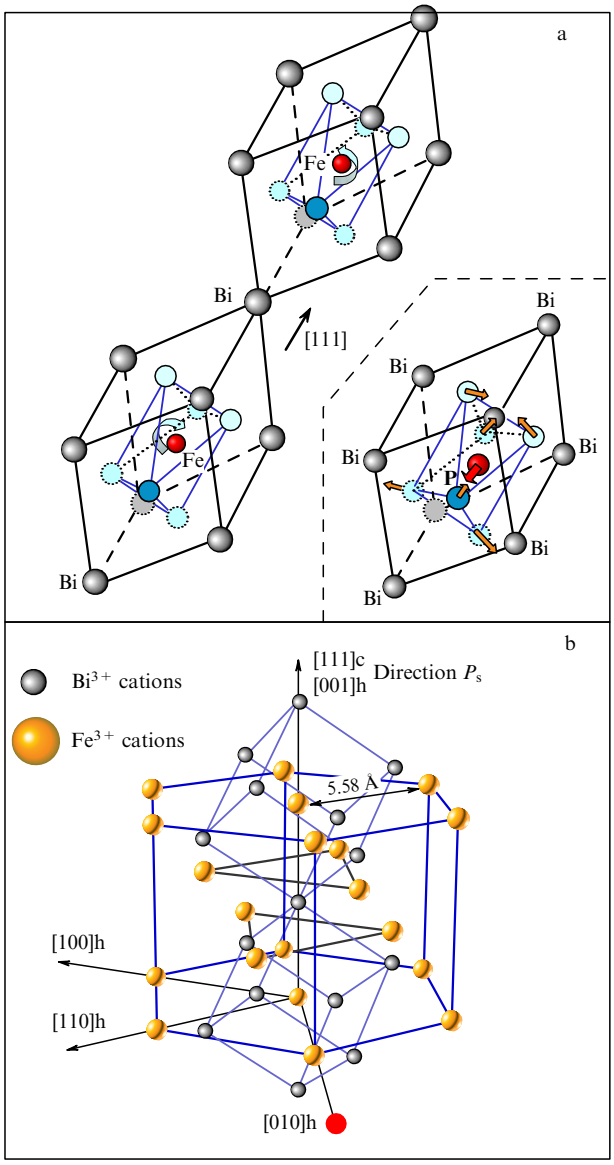

Figure 12. (a) Bismuth ferrite cell (rhombohedrally distorted perovskite cell) doubled via antiparallel rotation of oxygen octahedrons around the [111]-axis. (b) Bismuth ferrite cell in a hexagonal arrangement. Indexes 'c' and 'h' stand for 'cubic' and 'hexagonal', respectively.

surrounded by an oxygen octahedron with O ions arranged at the centers of the faces, and Bi ions occupying the vertices of a cube. The perovskite structure loses stability with a drop in temperature according to calculations [184, 185] and for $T < T_C$ turns into a structure with the $R3c$ symmetry group and a double unit cell along one of the cube diagonals [rhombohedrally distorted perovskite cell (Fig. 12a)] [186]. The atomic displacement occurs as follows: oxygen octahedrons in adjacent perovskite cubes of the bismuth-ferrite double cell turn clockwise and counterclockwise around the [111]-axis. Such 'antirotation' is accompanied by the displacement of iron and bismuth ions along the [111]-axis, with oxygen ions moving in the opposite direction; as a result, spatial inversion of the crystal becomes violated. This processes causes deformation of octahedrons that undergo enlargement of the region into which iron ions were displaced and contraction of the opposite side. These changes induce oxygen ion motion in the (111) plane toward the axis in one part of the octahedron, and away from it in the other (see inset to Fig. 12a).

The rotation of octahedrons through an angle of 14° plays the key role in this structural rearrangement [187]. The corresponding structural order parameter (or the phonon mode of the perovskite cell matching it) is the 'quasiaxial' vector **Φ** (staggered rotation) directed along the [111]-axis. The order parameter **Φ** is similar to the antiferromagnetic vector (staggered magnetization) in magnetism but remains T-even. Also, it is worthy of note that, from the standpoint of crystal symmetry, the 'quasiaxial' order parameter **Φ** is transformed according to the irreducible representation R_{25} at the R-point $\boldsymbol{\kappa}_{13} = (1/2, 1/2, 1/2)$ of the Brillouin zone in perovskite [188]. The second and third order parameters transform in accordance with irreducible representations at point Γ, i.e., in the center of the Brillouin zone.

Ion displacement along the [111]-axis is described by the polar order parameter and characterized by the electric polarization vector **P**. The third parameter **π**, corresponding to the displacement of oxygen ions in the (111) plane, is also polar; it makes a contribution to electric polarization along the [111]-axis. This inference ensues from the fact that oxygen ion displacement in the **π**-mode causes the oxygen octahedron to become asymmetric along the [111]-axis, i.e., compressed on the one side and extended on the other. As noted above, these three parameters of the $R3c$ ferrite phase are related to the corresponding unstable phonon modes of perovskite, known as 'frozen modes' of the perovskite structure.

There are also other unstable modes of the perovskite cell, in which polarization is directed along face diagonals or cube edges. However, such structural distortions in the crystal under consideration are energetically unfavorable [184, 185]; nonetheless, structures with such a polarization direction are known to realize themselves in films (see below).

Let us estimate electric polarization in bismuth ferrite based on a simple model of ion-localized point charges [189]. For the cell containing two Fe^{3+} and two Bi^{3+} ions depicted in Fig. 12a, polarization induced by ion displacements from the symmetric positions is expressed as

$$P_s = \frac{2 \times 3e}{V}(\delta_{Fe} + \delta_{Bi}) \approx 67\ \mu C\ cm^{-2}, \qquad (10)$$

where e is the electron charge, δ_{Fe} and δ_{Bi} are iron and bismuth ion displacements relative to their initial positions in the perovskite cell (total $0.0626c$ [190]), where $c = 2\sqrt{3}\,a$ is the height of the rhombohedral cell, $a = 3.96$ Å is the edge of the cubic lattice, and $V = 2a^3$ is the double perovskite cell volume. Oxygen ions in the arrangement used for the estimation were assumed to be undisplaced. Obviously, Born corrections to ion charges were neglected.

The initially measured values of polarization in bismuth ferrite crystals [169] proved to be ten times lower than estimate (10). Much higher values were obtained later, first in thin bismuth-ferrite films (Fig. 13) [191, 192], and then in bulk materials [193]; they were comparable to those in such classical ferroelectrics as barium titanate and lead zirconate titanate. It appears that an accurate measurement of electric polarization in bulky materials had been hampered before by the presence of leakage currents [194].

Polarization in bismuth ferrite single crystals of stoichiometric composition grown in a rather narrow pressure and temperature range was approximately estimated at 60 μC cm^{-2} [193], in excellent agreement with (10). Later on, more accurate calculations were undertaken using both

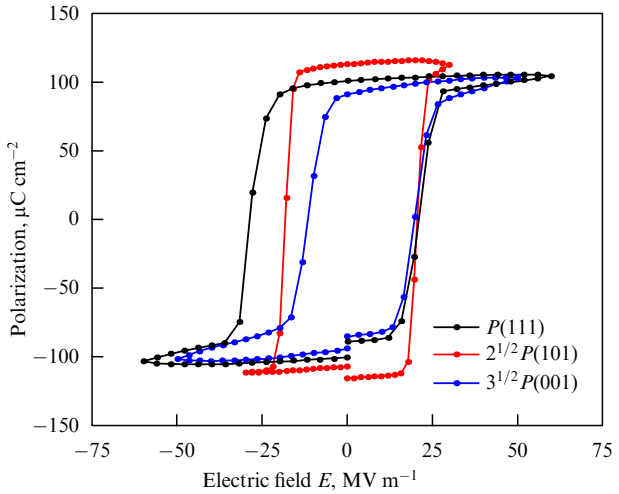

Figure 13. Electric polarization along the [111] direction recalculated from the normal polarization component for films on $SrTiO_3$ substrates with various crystallographic orientations (111), (101), (001). (Borrowed from Ref. [192].)

quantum-mechanical and first-principle (*ab initio*) methods [184, 185, 195]. The results are not significantly different from estimate (10).

As noted before, a structure in which polarization is directed along the principal cube diagonal [111] (the *c*-axis in a hexagonal arrangement) is most energy preferred in bulky crystals. Moreover, it remains stable under epitaxial stress in films grown on strontium titanate substrates with various crystallographic orientations (see Fig. 13) [192]. Another scenario is just as well realized in epitaxial films, namely the formation of a tetragonal crystalline structure [190, 196] with electric polarization along the [001] direction, in which a different mode is energy favorable. Polarization was reported to reach a record-breaking value of 150 μC cm^{-2} for ferroelectrics [197]. This was immediately noticed by Fujitsu Ltd., which announced the use of bismuth ferrite films in some components of ferroelectric random access memory (FRAM) [198].

Magnetization of bismuth ferrite depends first and foremost on the antiferromagnetic sublattice angularity, with the Dzyaloshinskii–Moriya interaction playing the key role:

$$F_{\mathrm{DM1}} = \mathbf{D}_1[\mathbf{L} \times \mathbf{M}]\,, \qquad (11)$$

where $\mathbf{D}_1$ is the axial T-even vector defined by antirotation $\mathbf{\Phi}$ of oxygen octahedrons, $\mathbf{L}$ and $\mathbf{M}$ are the vectors of antiferromagnetism and weak ferromagnetism, respectively, and $L^2 + M^2 = 1$.

Multiferroics with frustrated spatial inversion have an additional source of canting of sublattice magnetic moments:

$$F_{\mathrm{DM2}} = \mathbf{D}_2[\mathbf{L} \times \mathbf{M}]\,, \qquad (12)$$

caused by the presence of electric polarization $\mathbf{P}$ in the crystal [14].

While the F_{DM1} problem is pretty clear [199], the F_{DM2} interaction needs to be further investigated in detailed quantum-mechanical and experimental studies.

The magnetic symmetry of bismuth ferrite admits the existence of a linear ME effect, in addition to weak ferromagnetism [186, 199]. However, neither of these

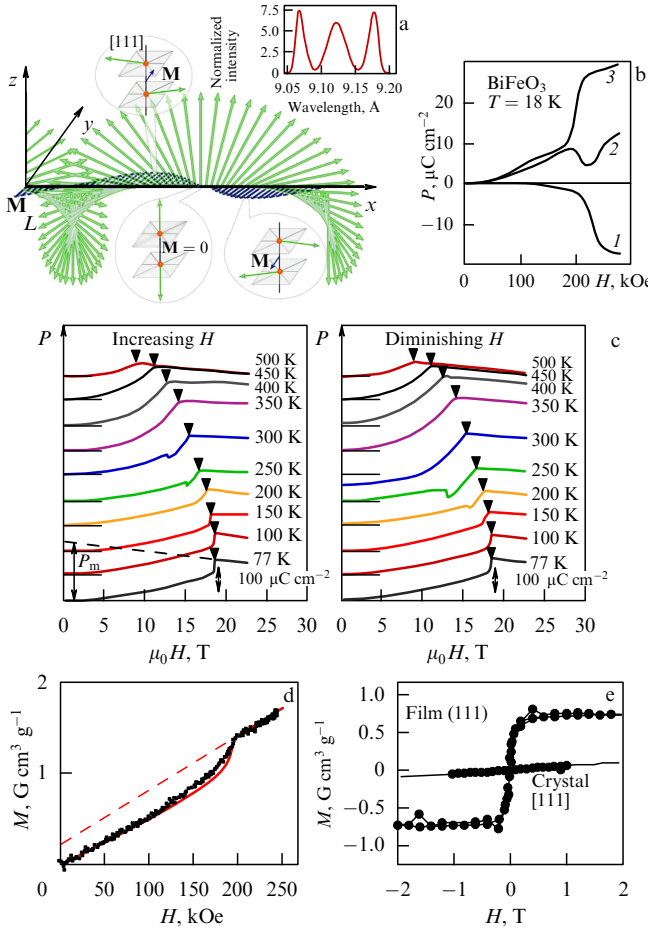

Figure 14. (a) Spin cycloid and the corresponding spin density wave in the perpendicular plane. The *z*-axis is oriented along [111], the *x*-axis along one of the second-order axes: [1$\bar{1}$0], [10$\bar{1}$], and [01$\bar{1}$]; insets at the bottom show the antiferromagnetic sublattices canting and the resulting vector of local magnetization at different points of the spin cycloid; inset in the top right corner depicts schematically a neutronogram [201]. Electric polarization anomalies in bismuth ferrite placed in strong magnetic fields: (b) magnetoelectric dependences in longitudinal geometry: *1* — $P_a(H_a)$, *2* — $P_b(H_b)$, *3* — $P_c(H_c)$ [114] (μ_0 is the permeability of vacuum); (c) jump of polarization $\mathbf{P} \parallel c$ in the magnetic field $\mathbf{H} \parallel c$ at different temperatures in growing and weakening magnetic fields (reproduced with generous permission of M Tokunaga [213]). (d) Manifestation of the weak ferromagnetic moment of bismuth ferrite in strong magnetic fields [171]. (e) Magnetization curves of bulky $BiFeO_3$ samples along [111] direction and thin films from the same material with substrate crystallographic orientation (111) [215].

phenomena could be observed for a rather long time — only a quadratic ME effect was established [200]. Early neutronographic studies demonstrated that the magnetic structure of a material was somewhat more complicated than simple G type antiferromagnetic ordering (spin staggered ordering). Broadening of the diffraction peak compelled suggesting the presence of spatial modulation of magnetizaton with a large period [186]. Higher-resolution neutronographic measurements revealed satellite diffraction peaks corresponding to the spin cycloid with a period of 62 nm [201], lying in the plane normal to the basal plane (Fig. 14a) and running along one of the three second-order symmetry axes. The source of the spin cycloid is the flexomagnetoelectric interaction [see formula (8)] characterized by the surface energy $\gamma P_s \sim 0.6$ erg cm^{-2}, due to which spontaneous electric polarization induces spatial spin mod-

ulation [120]. The presence of the cycloid accounts for the zero values of volume average magnetization and magnitudes of the ME effect: because magnetization determined by weak ferromagnetism is proportional to the projection of the vector **L** of antiferromagnetism onto the basal plane, the spin cycloid is accompanied by a spin density wave [171, 202]. Interestingly, this wave was detected by the small-angle neutron scattering technique [203] only in 2011.

The spin cycloid being an interesting subject in itself, most studies in the late 20th century were focused on the dependence of its structure and period on temperature, magnetic anisotropy, and impurity concentration [204, 205]. This issue remains relevant up to the present [202, 206–210]. Moreover, the spin cycloid was found to be suppressed in high magnetic fields [211–213] (Fig. 14b, c); this phenomenon manifested itself in effects that were formerly masked by the cycloid, viz. a linear ME effect (Fig. 14b), induction of the toroidal moment, and emergence of spontaneous magnetization (Fig. 14d) [171].

Although bismuth ferrite belongs to type 1 multiferroics (i.e. its ferroelectric ordering proceeds independently of the magnetic one at elevated temperatures), only a small part of its polarization (less than 0.01%) in magnetically ordered state is due to spatial spin modulation (see Section 2.3), as becomes apparent only after the cycloid disappears (Fig. 14a) [202, 212].

Despite the fundamental significance of the above-mentioned phenomena, the practical application of a 'hidden magnetoelectric' was out of the question, since it occurred in extremely high fields ($\sim$ 200 kOe). The situation changed drastically after the advent of bismuth ferrite-based thin-film materials [191, 192, 197, 214–217]. The spin cycloid is absent in $\sim$ 100-nm thick films, which enabled observation of both weak ferromagnetism ($\sim$ 5 G) even in a moderate magnetic field of 100 Oe [215] (Fig. 14e) and a 10 ps m^{-1} linear ME effect [218] (taking account of dielectric constant of the material $\varepsilon = 50$ [19] at $T \approx 300$ K, it corresponds to 15 mV cm^{-1} Oe^{-1}, i.e., the value close to that in the classical magnetoelectric Cr_2O_3).

Piezoelectric effects are also high in magnitude (a few dozen pm V^{-1}), which allows using bismuth ferrite films to measure mechanical stress in microelectromechanical systems [219]. We note in addition that a strong piezoelectric effect was theoretically predicted [220] to enhance the linear ME effect, however, the huge magnitudes of the latter and of magnetization anticipated in an early study on thin bismuth ferrite films [191] were not confirmed by subsequent investigations.

Magnetoelectric interactions in thin bismuth ferrite films manifest themselves not only in the form of linear and quadratic ME effects but also in a number of other effects. For example, an electric field can be applied to switch over magnetization of a material. Symmetry considerations seemingly suggest that the switching of electric polarity must not lead to switching the magnetic order parameter, because electric and magnetic vectors have different transformation properties. This fundamental constraint can be overcome by assuming that the act of switching is not necessarily reduced to rotating either the magnetic or electric vector by 180°. When electric polarization in bismuth ferrite undergoes reorientation from one cube diagonal to the other, both the antiferromagnetic vector and the related magnetization vector turn together with polarization vector due to magnetoelectric coupling, which leaves their relative orientation unaltered (Fig. 15a, b). It is in this way that the effect of electric switching of the magnetic state in bismuth ferrite films was demonstrated in 2006 [221]. Using a 600-nm thick film, the authors obtained an electric field of the desired strength by applying a voltage of 10 V. Importantly, the effect was observed at room temperature, which is crucial for electronic device applications. The difficulty arises, however, from the fact that magnetic moments of antiferromagnetic sublattices are mutually compensated and that overall magnetizaton of bismuth ferrite is rather low ($\approx$ 5 G). It can be enhanced by depositing a ferromagnetic layer over a bismuth ferrite crystal, which are coupled by exchange interaction through the common interface. This approach was proposed in earlier studies to produce ME materials with a strong ME effect based on Cr_2O_3/Pt/Co/Pt heterostructures [222, 223] and manganite $YMnO_3$/Py (permalloy) [224]. By switching over the electric polarization of bismuth ferrite and thereby changing anisotropy axes, it is possible to turn the spins of antiferromagnetic sublattices and thus control high magnetization (1500 G) in the ferromagnetic CoFe layer by taking advantage of the exchange coupling between the layers [225, 226].

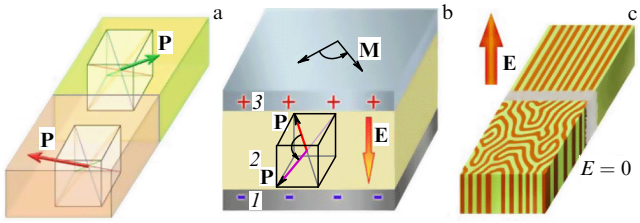

Figure 15. (a) Switching of the magnetic order parameter by an electric field: two ferroelectric domains are separated by the domain boundary in bismuth ferrite. (b) Schematic of a heterostructure: *1* — electrode, *2* — ME layer coupled with ferromagnetic metal layer *3* by an exchange interaction. Variations of voltage polarity switch over sublattice spins in antiferromagnetic layer *2*, which leads to the switching of magnetization in layer *3*. (c) Transformation of the labyrinth magnetic domain structure into a stripe domain one under the effect of an electric field (see Ref. [227] for a description of the experiment).

Another strategy for achieving the same effect consists in substituting rare-earth ions for bismuth atoms. This approach does not require using a ferromagnetic layer, since the resultant material possesses its own magnetization (more details on substituted compositions are provided below). The same controling voltages ($\approx$ 10 V) transformed a labyrinth magnetic domain structure into a stripped one [227] (Fig. 15c). The possibility of controling magnetization of materials at room temperature by an electric field is of interest in the context of their use in elements of computer memory with electric recording and magnetic read out [179].

Bismuth ferrite is a highly promising candidate for the formation of a dielectric barrier in spintronic devices based on tunnel transition [177]. Bismuth ferrite exhibits a rhombohedrally distorted perovskite structure similar to that into which certain known magnetic halfmetals crystallize, which allows them to be combined with each other in epitaxial heterostructures. Reference [177] describes experiments with two-layer structures of a halfmetal $La_{2/3}Sr_{1/3}MnO_3$ and bismuth ferrite grown on a strontium titanate $SrTiO_3$ (001) substrate. Investigations into the structural, electric, and magnetic properties of these heterostructures gave evidence

that bismuth ferrite retains its electric and ferroelectric properties in films as thick as 5 nm; the same refers to the magnetic properties of the halfmetal.

Some progress was achieved in checking the compatibility of bismuth ferrite with traditional silicon-based electronics by growing epitaxial bismuth ferrite films on silicon substrates. Although the aforementioned perovskites (strontium titanate [228] or $La_{2/3}Sr_{1/3}MnO_3$ [229]) are usually utilized as a buffer layer, recent publications report on growing bismuth ferrite films directly on the silicon substrate by means of pulsed laser deposition [219] and the sol gel method [230].

The extraordinary properties of bismuth ferrite-based thin-film materials are explained to a large extent by the emergence of mechanical stress associated with film growth. This fact stimulated a string of research on bismuth ferrite properties, both hydrostatic (isotropic) and anisotropic, at high pressures.

As shown in Ref. [231], even a small mechanical stress of about 7 MPa may be sufficient to remove degeneracy in the basal plane with respect to the direction of spatial modulation, thus leading to a turn of the spin cycloid plane. It is therefore natural to expect that high pressure may destroy the spin cycloid. A series of structural phase transitions occur at an extremely high pressure; namely, a rhombohedrically distorted phase transforms into the monoclinically distorted perovskite phase at 3.5 GPa, and into orthorhombic and cubic phases at 10 GPa [232] and 45 GPa [233], respectively. The latter transition is accompanied by anomalies in the magnetic, optical, transport, and structural properties of the crystal [234, 235].

Partial replacement of ions in $BiFeO_3$ crystals by impurities may serve as a sort of mechanical pressure. Studies on the impurity composition of bismuth ferrite-based materials initiated in the 1990s [189, 236] currently constitute the bulk of research concerning multiferroics. Their comprehensive consideration is beyond the scope of the present review, which is confined to a discussion of the most important issues (see Refs [173, 174] for more details).

Bismuth ferrite-based compositions can be divided into two main groups, with substitutions of bismuth and iron ions. In the former case, rare-earth impurities are usually utilized, and the properties of bismuth ferrite become more like those of orthoferrites as their percentage increases [237, 238]. When the amount of admixtures is relatively small (up to 30%), their substitution for bismuth ions lowers the critical field of spin cycloid suppression [239, 240]. In certain cases, the cycloid may be suppressed even in the absence of the magnetic field [189, 236, 240–242]. The substitution of alkaline-earth elements (Ca^{2+}) for bismuth ions suppresses a spatially modulated structure even at their 3% concentration [243]. One of the most commonly used compositions is bismuth ferrite with bismuth ions substituted by neodymium, $Bi_{1-x}Nd_xFeO_3$ ($x = 0-0.15$), which improves the dielectric, piezoelectric, and ferroelectric properties of the material [196, 244–246]. The piezoelectric effect is further enhanced in compositions with the substitution of 14% bismuth ions by samarium near the morphotropic phase boundary where crystallostructural instability evolves [247]. A similar phenomenon is evidenced in classical piezoelectrics like lead zirconate titanate, but bismuth ferrite-based materials have the important advantage of being free of toxic lead. Substitution by Tb ions allows substantially increasing saturation magnetization M_s (up to $4\pi M_s = 600$ G) [248].

Replacement of iron ions by transition element ions with similar ionic radii, Ti^{4+} and Ni^{2+}, increases and decreases the resistivity of the material, respectively, by several orders of magnitude. Tetravalent titanium ions decrease the number of oxygen vacancies and enhance dielectric properties of the substances; vice versa, bivalent nickel ions increase the concentration of oxygen vacancies and thereby improve conductivity [249]. In addition, the substitution of Ti ions for Fe ions leads to the appearance of weak ferromagnetism in the spontaneous state [240] and, consequently, to spin cycloid suppression.

In a series of studies [177, 250–253], bismuth ferrite was employed as a base for producing nanostructures, viz. nanotubes 250 nm in diameter [250], epitaxial heterostructures integrated into spintronic devices [177], nanocomposite materials consisting of hematite α-Fe_2O_3 layers (as a magnetostrictor), and bismuth ferrite (as a piezoelectric) [251]. Such materials, as well as nanocomposites in the form of columnar structures of magnetostrictive materials integrated into a bismuth ferrite matrix [252], exhibit a pronounced ME effect of 20 mV cm^{-1} Oe^{-1} [253] that is a kind of 'product' of magnetostriction and the piezoeffect.

It should be emphasized that, despite a broad band gap (2.7 eV) in bismuth ferrite, it exhibits semiconducting properties at room temperature, and even turns into a well-conducting material in the domain boundary region (as mentioned in Section 2.6). On the one hand, it hampers the utilization of bismuth ferrite in devices where dielectric and ferroelectric properties of the material are essential [achieved by the replacement of bismuth or iron ions by admixtures (see above)]. On the other hand, the unique semiconductive properties of bismuth ferrite-based materials call for special investigations. Suffice it to mention the possibility of changing the type of conductivity and even inducing the p–n transition in Ca-doped bismuth-ferrite films by applying an electric field [254]. In this case, calcium ions and oxygen vacancies function as acceptor and donor impurities, respectively. The effects of Ca ions and oxygen vacancies are mutually compensating in thermodynamic equilibrium, with bismuth ferrite behaving as an insulator. However, positively charged oxygen vacancies undergo redistribution in the sample volume under the action of an electric field (Fig. 16a). They concentrate near the cathode to form a region with n type conductivity, outside of which p type conductivity is established, with the resistivity decreasing to $\sim 10^2\ \Omega$ cm.

The semiconducting properties of bismuth ferrite also manifest themselves in photogalvanic effects. Optical emission induces photocurrent in bismuth ferrite, the direction of which depends on the direction of electric polarization [255, 256]. The quantum yield of the photoeffect in bismuth ferrite is not inferior to that in semiconductors traditionally utilized in photocells [180]. As shown in Ref. [257], an important role in the mechanism of the photogalvanic effect is played by ferroelectric domain boundaries at which the arising electric field effectively separates electron–hole pairs produced and thereby considerably diminishes the recombination rate. Although the photoinduced potential difference at each boundary is not very high (~ 10 mV), photoelectric electromotive forces (EMFs) of domain boundaries are summed upon circuit closure and the total EMF of the domain structure extending across the span of thousands of periods may reach a few dozen volts, thus much exceeding the energy gap width. One consequence of photogalvanic phenomena in

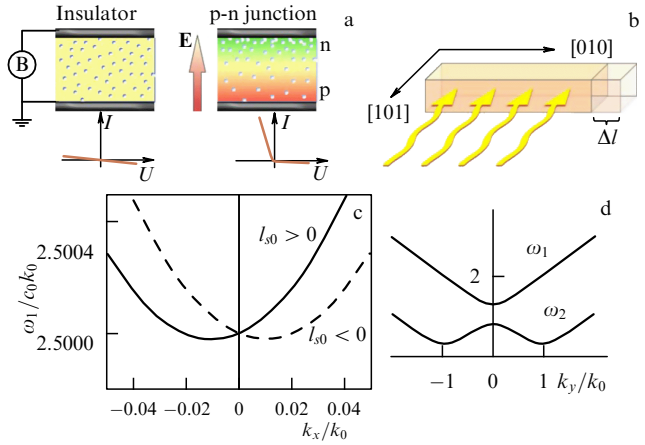

Figure 16. (a) Redistribution of oxygen vacancies (white voids) in a sample of bismuth ferrite under the action of an electric field in excess of the critical one (6×10^5 V cm^{-1}) results in local decompensation of donor and acceptor impurity concentrations (oxygen vacancies and calcium ions, respectively) and in the formation of the p-n junction [254]. (b) Photoinduced striction of a bismuth ferrite sample. Spin excitation spectra of magnonic modes for spin waves propagating in the basal plane (normal to polarization **P**) [261]: (c) in longitudinal geometry $\mathbf{k} \| \mathbf{l} \perp \mathbf{P}$ (to illustrate nonequivalence of spin wave propagation along and opposite the antiferromagnetic vector **l**), and (d) in transverse geometry $\mathbf{k} \perp \mathbf{l} \perp \mathbf{P}$ (a minimum arises for one of the modes at a point corresponding to cycloid wave number k_0).

bismuth ferrite is photostriction observed in it, i.e., a photoinduced change in the sample size [258]. Photostriction had been observed before in ferroelectrics, polymers, and semiconductors, but never in magnetic substances.

At a certain position of the light source (Fig. 16b), the sample measurably extends in the crystallographic [010] direction. The elongation per unit length caused by the light of a 100-watt bulb is on the order of 10^{-5}. The authors of Ref. [258] attribute bismuth ferrite photostriction to the joint action of the photogalvanic effect and the inverse piezoelectric effect. Characteristically, the degree of photostriction depends on the applied magnetic field — such dependence had not been observed before. Photostriction linearly decreases with the strength of the applied magnetic field (by 30% in a field of 1.5 T).

Bismuth ferrite is a promising material for applications not only in the optical range but also in the IR (to fabricate plasmonic superlenses [181]), gigahertz, and terahertz ranges. A change in dispersion of spin waves during their propagation in bismuth ferrite under the action of an electric field was predicted in a series of publications [259–261]. The linear ME effect is manifested in nonreciprocal effects (Fig. 16c), and inhomogeneous ME interaction in the emergence of a dispersion dependence minimum at the spatial frequency corresponding to cycloid wave number $\mathbf{k}_0$ (Fig. 16d). It reflects the development of instability with respect to transition from the homogeneous antiferromagnetic state (inherent in bismuth ferrite films) to the spatially modulated one (characteristic of bulky single crystals). Electric tuning of the magnonic mode frequency by more than 30% was observed in bulky samples [262].

Researchers have continued being surprised by a number of miscellaneous properties of bismuth ferrite throughout the last decade. The revival of interest in bismuth ferrite after the discovery of its ferroelectromagnetic and magnetoelectric properties stimulated numerous investigations that revealed new effects and promoted deeper understanding of not only magnetoelectric phenomena but also those in the adjacent field of the physics of ferroelectrics and semiconductors.

3.2 Other high-temperature magnetoelectric materials

Setting aside numerous bismuth ferrite derivatives, there are rather few materials displaying ME properties at room temperature. These are the aforementioned Cr_2O_3 (the first magnetoelectric discovered) [26], hexaferrites (spiral multiferroics) [124, 125, 263], iron–gallium oxides [264], lead ferrotantalates, ferronyobates, ferrotungstates [156], etc. (see Table 1). Iron garnet $R_3Fe_5O_{12}$ films need to be specially mentioned. The symmetry group of these crystals has a symmetry center that forbids linear-in-electric-field effects. Indeed, iron garnet crystals exhibit an ME effect quadratic in the electric field [272] and a quadratic electromagneto-optical effect (a change in the Faraday rotation angle of the light polarization plane under the action of an electric field) [85].

In addition, iron garnet films exhibit the linear electromagnetooptical effect [273] due to the central symmetry violation. These films are also remarkable for the possibility of easily observing magnetic domains by magnetooptic techniques, making them convenient objects for the study of electric polarization in micromagnetic structures arising from inhomogeneous ME interactions.

3.3 Electric polarization of domain boundaries in iron garnet films

Spatial modulation of magnetization occurs not only in spiral multiferroics but also in any magnetic substance tending to be split into domains. The interdomain boundaries (domain walls) are regions in which the magnetization vector gradually rotating when passing from one domain to another. In other words, domain boundaries are magnetic spiral-solitons categorized into two classes, depending on the rotation type: Bloch walls corresponding to a helicoid, and Néel walls symmetrically analogous to a cycloid (see Section 2.3) (Fig. 17a, b). As cycloids can be associated with certain electric polarizations, a possibility appears to control the micromagnetic structure by means of an electric field. It is important in the context of practical applications that these effects can be observed under the same conditions as the micromagnetic structure, i.e., at room temperature as well.

Notably, the term 'inhomogeneous magnetoelectric effect' corresponding to interaction (8) was introduced by Bar'yakhtar et al. [106] in connection with examining domain boundaries whose ME properties were later considered in theoretical studies [106–109, 111, 112, 274–278]. Of special note is the universal character of electric polarization phenomenon attributable to a certain type of micromagnetic inhomogeneities; in fact, such polarization emerges in any magnetic insulator, even in a centrally symmetric one [109]. Surprisingly, there has until recently been no experimental evidence of the electrical properties of domain boundaries.

In 2007, the motion of domain boundaries in iron garnet films in inhomogeneous electric field was detected; the latter was induced by a tapered electrode positioned near the domain boundary [157] (Fig. 17c, d). As mentioned in Section 2.5, domain boundaries in iron garnet films have a single direction of magnetization rotation. This makes itself evident in the identical electric polarity of domain boundaries: all of them are attracted to a positively charged needle

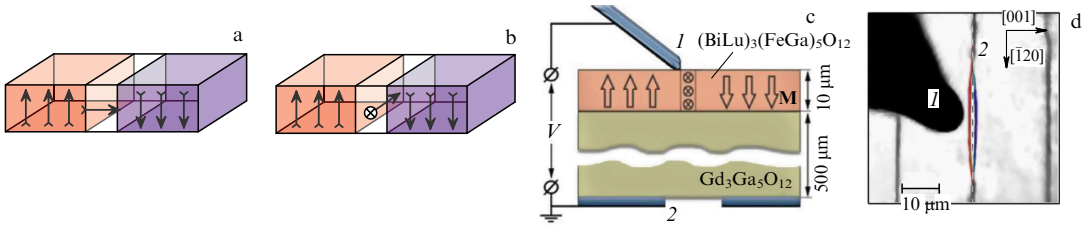

Figure 17. Two types of domain boundaries: (a) Néel wall, and (b) Bloch wall. (c) Schematic of the experiment on the displacement of domain boundaries by an electric field: *1* — the tip from a nonmagnetic metal (copper, gold), *2* — the grounded electrode; (d) Magnetooptic image of a film in transmitted light: part of domain boundary *2* near electrode *1* deflects from an equilibrium position (dashed straight line), being attracted to the tip at a positive electrode potential (solid line left of the dashed one) and repulsed from it at a negative potential (solid line right of the dashed one) [158].

Table 1. High-temperature magnetoelectrics and multiferroics (T_{eo} and T_{mo} are the temperatures of electric and magnetic ordering, respectively).

Compound	Polarization, μC cm^{-2}	Magnetization*	ME effect, CGS	T_{eo}, K	T_{mo}, K	References
Cr_2O_3	Absent	Absent	10^{-3}	—	307	[3]
$Ga_{2-x}Fe_xO_3$		42 emu g^{-1}	10^{-2}	—	250 – 280	[264]
$SrSm_2Nb_2O_9$	4×10^{-2}	~ 2 emu g^{-1} (9 G)	—	> 300	> 300	[265]
$BaFe_{0.3}Zr_{0.7}O_{3-\delta}$		10 G	—	> 300	> 300	[266]
$Sr_3Co_2Fe_{24}O_{41}$	10^{-3}	20 μ_B/f.u.	5×10^{-2}	670	670	[124, 125]
$SrCo_2Ti_2Fe_8O_{19}$	10^{-3}	30 emu g^{-1}	5×10^{-2}	420	740	[263]
$In_xFe_{0.5}Mn_{0.5}O_3$	1	0.1 μ_B/f.u.	—	> 670	250 – 325	[267]
$NiBi_2O_4$	2	0.03 emu g^{-1} (~ 0.05 G)	—	> 630	> 630	[268]
$Bi_4(TiFe_2)O_{12-\delta}$	3	0.01 emu g^{-1}	—	> 300	> 300	[269]
$(Sr, Co)Bi_2Nb_2O_9$	10	4 G	—	> 300	> 300	[270]
$TbFe_3(BO_3)_4$	Paraelectric at T above $T_N = 40$ K	Antiferromagnet	5×10^{-4} (linearized dependence for the quadratic effect at $H \approx 1$ T)	40	40	[271]
Iron garnet films $R_3(Fe_5Ga_5)O_{12}$	Absent	5 – 100 G	10^{-2} (assessment from the electro-magneto-optical effect) [273]	—	400 – 700	[272, 273]
* f.u. stands for the formula unit.						

tip, and repulsed from a negatively charged one (Fig. 17d) [157, 158].

This effect is especially pronounced at the heads of magnetic domains (Fig. 18a), which allows measuring the velocity of propagation of domain boundaries and its dependence on the electric filed (Fig. 18b). By comparing the results of measurements in electric and magnetic fields, it is possible to estimate the effective magnetic field acting on the domain boundary. A voltage of 500 V (corresponding to an electric field strength of 1 MV cm^{-1} at the needle tip) exerts the same effect as a magnetic field of 50 Oe.

As shown in recent experiments, electric polarization of domain boundaries in iron garnet films can be switched over by applying a magnetic field of the order of 50 Oe [155]. It is supposed that a magnetic field normal to the domain boundary alters its micromagnetic configuration so that the magnetization vector in the center of the domain boundary becomes parallel to the field vector, with the result that the magnetic film passes into a new state with the opposite direction of magnetization rotating in neighboring domain boundaries (Fig. 18c, d).

As the direction of the magnetic field changes to the opposite one, the direction of magnetization rotation in the domain boundaries changes, too; it is apparent as the switching of electric polarization in the domain walls (Fig. 18e).

3.4 Magnetic vortices and electric polarization

Magnetic vortices are considered to be an alternative to magnetic domains for the representation of binary information [279], because they do not induce stray fields that affect their neighbors and serve as a serious limiting factor for increasing record density. However, control of magnetic vortices remains challenging. A few approaches to addressing this problem have been proposed, including remagnetization either by a pulsed magnetic field [280] or by spin current pulses [281]. Unfortunately, these methods imply high electric current density and the presence of thermal losses.

In this context, the flexomagnetoelectric effect provides an interesting option for controling magnetic vortices by means of a static electric field. A magnetic vortex may be considered as a spin cycloid terminated in itself, in which the

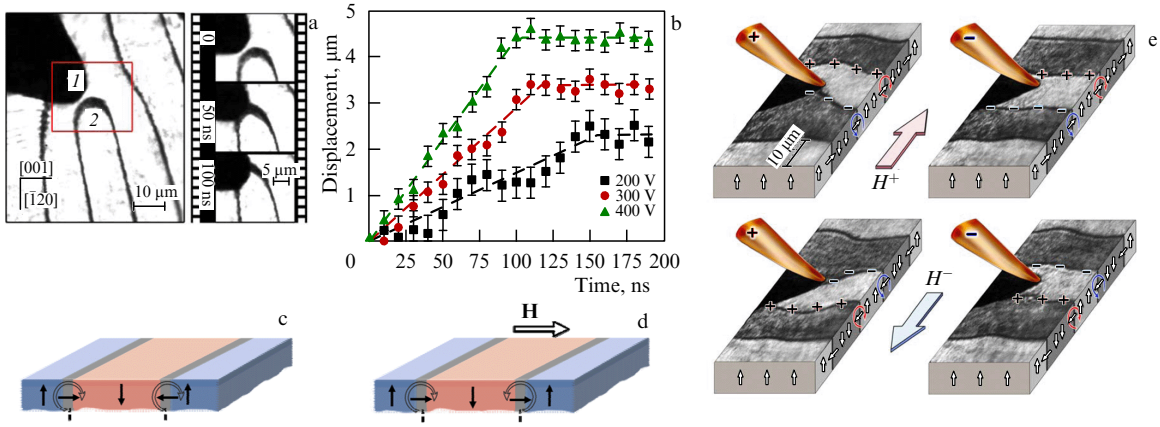

Figure 18. (a) Movements of the magnetic domain head resulting from an electrostatic impact: original configuration (*1* is a tip electrode, *2* is a strip domain head) and sequential head positions at different time moments. (b) Time dependence of domain boundary displacement at different electrode potentials [158]. Schematic representation of micromagnetic structure in iron garnet films: (c) spontaneous state, (d) the state in an external magnetic field (for display purposes, the size of domain boundaries is enlarged). (e) Dependence of electric polarity of magnetic domain boundaries on their micromagnetic structure rearranged by the magnetic field. The combined pictures of a magnetooptical image (top layer) and schematic representation of magnetization distribution (arrows below) are shown. Opposite directions of magnetization rotation in adjacent walls appear in interactions with an electrically charged probe as surface electric charges with opposite signs [155].

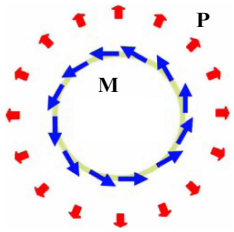

Figure 19. Vortical distribution of magnetization giving rise to the radial distribution of electric polarization.

modulation direction varies from one point to another (Fig. 19) [282]. Then, the total electric polarization of such a vortex is zero: the existing electric properties do not manifest themselves externally. Zero polarization, however, does not mean the absence of electric properties, because the divergence of **P** corresponds to a bound electric charge $\rho(\mathbf{r})$:

$$\rho(\mathbf{r}) = -\mathrm{div}\,\mathbf{P}(\mathbf{r})\,, \tag{13}$$

where $\mathbf{P}(\mathbf{r})$ is defined by formula (9). This gives the opportunity to control magnetic vortices by means of an electric field.

A nonuniform electric field, such as that induced by the cantilever tip of a probe microscope, may create a vortex or antivortex state in a magnetic nanoparticle, depending on the electric polarity of the needle tip (Fig. 20a, b). This allows the system in question to be considered as a prototype electrically switchable element of magnetic memory with two logical

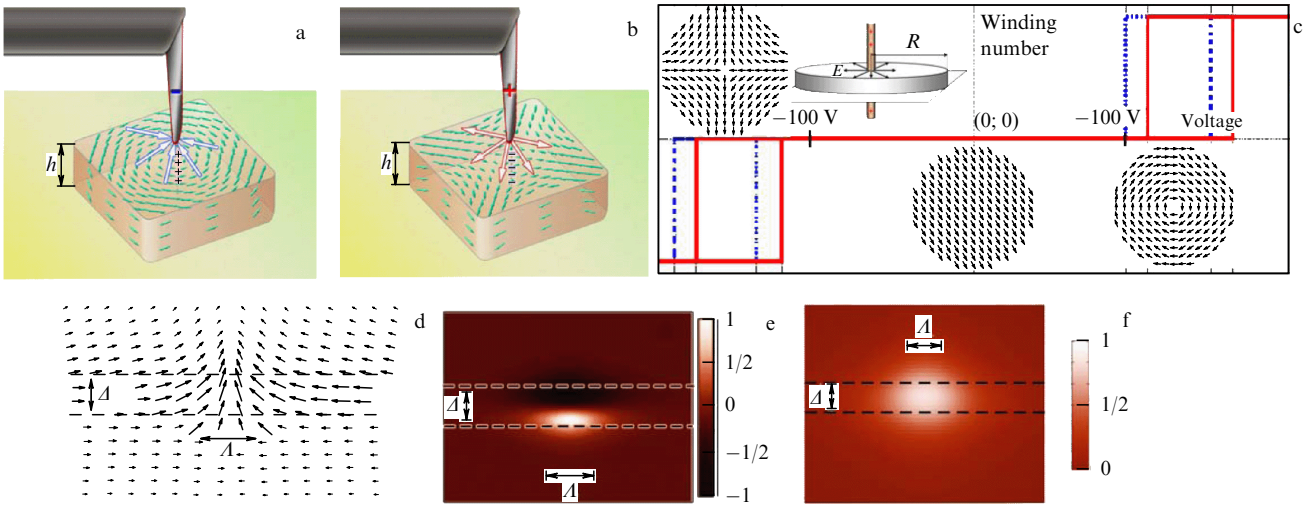

Figure 20. Electric switching of the topological charge of the magnetic vortex in a magnetic nanoparticle: (a) magnetic vortex, and (b) magnetic antivortex. (c) Hysteretic cycle for switching over the vortex and antivortex in an electric field; insets display (from left to right) micromagnetic distributions in antivortex, homogeneous, and vortex states; hysteresis at magnetization $M_s = 5$ G (solid line) and $M_s = 50$ G (dotted line); $R = 100$ nm. Vertical Bloch line in the domain wall separating domains with vertically oriented magnetization (top view of the film): (d) micromagnetic distribution (the domain wall with characteristic width Δ is shown by the dashed line, and the Bloch line characterized by the width Λ is in the center; (e) electric charge density distribution calculated from formula (13) [290], and (f) surface charge density near the Bloch line, equal to the normal component of electric polarization.

states [283]. We note that the antivortex state of a magnetic particle (Fig. 20b) cannot be realized under ordinary conditions, because it is associated with an additional magnetostatic energy attributed to the formation of magnetic charges at the particle periphery. There are few reports observing magnetic antivortices in the metastable state of cruciform magnetic nanoparticles [284, 285].

Nevertheless, theoretical estimates [283] and micromagnetic calculations suggest that the magnetic antivortex state is possible to stabilize in an electric field. The computations were done with the use of the SpinPM micromagnetic simulation package [286] modified to take into account the contribution of flexomagnetoelectric interaction (8) to the effective magnetic field [287].

Figure 20c gives the results of numerical calculations of the hysteresis cycle in the electric field for a 200-nm magnetic particle with parameters typical of magnetic insulators with magnetic ordering temperature above room temperature, viz. exchange interaction constant $A = 3 \times 10^{-7}$ erg cm^{-3}, magnetization $M_s = 5-50$ G, and magnetoelectric constant $\gamma = 10^{-6}$. It was assumed that the source of the electric field is a 10-nm wire passing through the disk center. The absolute value of this field necessary for an antivortex to form is higher than that for a vortex, the reason being that the magnetostatic energy of the antivortex state is higher. The picture becomes more symmetric in materials with lower saturation magnetization (Fig. 20c, solid line).

Let us consider vortices formed in Bloch domain boundaries at the sites where rotation direction (vertical Bloch lines) changes. These topological perturbations may result either from the action of a magnetic field or from local heating of the material by a focused laser beam [288]. Figure 20e illustrates the micromagnetic distribution in a vertical Bloch line, while associated bulk and surface charge densities are shown in Fig. 20e, f, respectively. Electric polarization related to the Bloch lines is manifested as a change of their position under the action of an electric field [289–291].

4. Potential applications of magnetoelectric materials

Magnetoelectric materials open up wide prospects for applications in the field of information and energy-saving technologies. These materials may form the basis for manufacturing magnetic sensors, capacitance electromagnets, elements of magnetic memory, nonreciprocal microwave filters, and other devices operated in the absence of passing through them direct currents and related thermal losses. Certain applications, e.g. sensors, are already integrated into routine practice, others continue to be developed, and still others exist only mentally. Despite the most versatile degree of the practical utility of applications, we thought it appropriate to consider many of them here in an attempt to gain the attention of researchers to this promising field.

4.1. Magnetic field sensors

Magnetic sensors are the most obvious and well-substantiated embodiment of the idea of practical application of the ME effect [51–53, 292–295]. There is a broad variety of constant and alternating field sensors built around composites and having a sensitivity greatly in excess of that of sensors based on the Hall effect and giant magnetic resistance (up to 1 pT in a frequency range of $10^{-2}-10^{3}$ Hz [293]). Also, they are vastly cheaper than SQUIDs, which allows these sensors to be used even for such purposes as magnetoencephalography and magnetocardiography.

An optimal sensor geometry is chosen taking account of the magnetic field configuration. The vortex field created by a current-carrying conductor is detected using a sandwich structure comprising two rings made from the magnetostrictive material Terfenol-D and a piezoelectric ring placed between them [294] (Fig. 21). At the same time, a uniform field is more efficaciously detected with a structure of piezoelectric fibers aligned parallel to the field and inserted between two magnetostrictive layers [292]. The ME sensors can be readily miniaturized by photolithographic processing, taking advantage of their planar geometry. This permitted the authors of Ref. [295] to propose an alternative method of magnetic probe microscopy to measure directly magnetic field components rather than the force impacting the magnetic needle tip (Fig. 21c).

4.2 Electrically switchable permanent magnets

Magnetoelectric interactions in matter result not only in emerging magnetic field-induced electric polarization but also in an inverse effect, i.e., emergence of magnetization under the action of a constant electric field. This phenomenon can be employed to design instruments combining useful properties of electromagnets (the possibility of controling the strength and direction of a magnetic field) and permanent magnets (the absence of energy consumption for the maintenance of electric current passage). Direct and inverse effects in composite materials are not identical to each other, in contrast to those in single-phase media [296, 297]. Coefficients of the inverse ME effect in traditional layered composites are ~ 0.1 G cm V^{-1} [298].

Of interest in this context is an earlier idea to create an artificial magnetoelectric, the Tellegen medium (see Section 2.1). It was eventually realized in the form of one of the first technologies for electronic ink [299] and liquid crystal

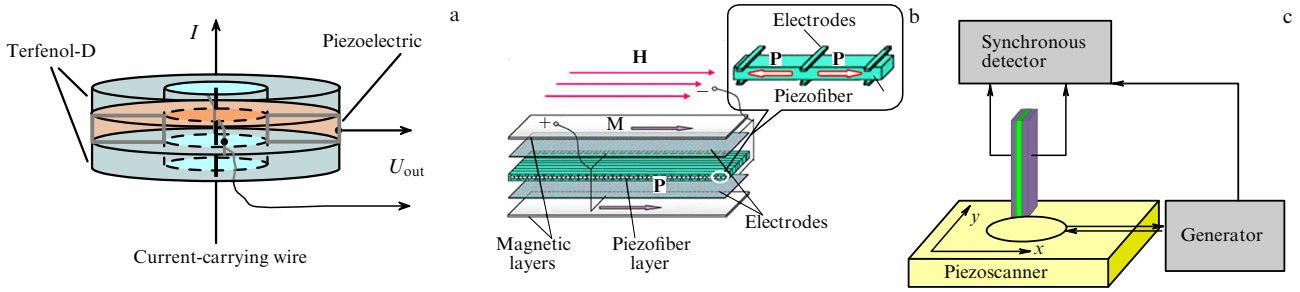

Figure 21. Magnetic field sensors for measuring (a) vortex field from the current [294], and (b) uniform field in the plane [292]. (c) The probe of a magnetoelectric scanning probe microscope [295].

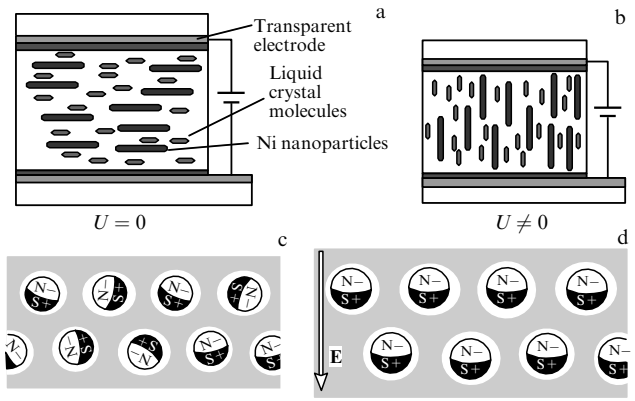

Figure 22. An example of composite magnetic insulators possessing ME properties. (a) A liquid crystal cell containing suspended oblong Ni nanoparticles. (b) Reorientation of molecules and nanoparticles bound to them in an electric field. (c) A piece of gyricon (electronic paper) with particles-dipoles freely rotating in fluid-filled microcavities: + and − signs denote electric poles, S and N are the magnetic poles. (d) Particle reorientation under the action of an electric field is responsible for the emergence of a nonzero resultant magnetic moment.

display elements with implanted magnetic nanoparticles [300]. Application of an electric field to such elements causes particle reorientation, thus opening up the possibility of controling magnetization of the medium without energy consumption for the maintenance of electric current. Display elements are based on implanting liquid crystal molecules (Fig. 22a, b), and electronic paper is based on polyethylene microspheres freely rotating in fluid-filled cavities (Fig. 22c, d).

Although the magnetic fields generated in such devices are thus far not very high (a few milligauss for electronic paper, and several gauss for liquid crystals), these magnitudes can be increased by the adequate combination of admixtures. A more serious drawback of these systems lies in their low operation speed (characteristic switchover time averages a few milliseconds for liquid crystals, and up to 1 s for electronic paper). For this reason, Tellegen media are of lower value for solid-state microelectronic applications than either layered composites or single-phase ME materials. However, they may be useful for applications in microfluidics (a branch of hydrodynamics dealing with the creation of 'liquid robots' for automatic performance of chemical and biochemical operation), microelectromechanical systems, and, probably, plastic microelectronics.

4.3 Magnetic memory and spin electronic devices

Computer memory based on ME materials was proposed as early as 1965 [16]. Data bits in such materials might be antiferromagnetic domains creating no demagnetizing fields; being simultaneously ME domains, they undergo polarization in an external magnetic field (Fig. 23a).

An important constraint on such memory is imposed by the complicated recording procedure, which includes heating up to $T > T_N$ and cooling in the presence of magnetic and electric fields to $T < T_N$. At the same time, magnetoelectrics might serve as the main materials for permanent read-only-memory (ROM) storage devices with a high operation speed; their magnetoelectric coefficient remains unaltered at frequencies up to 100 GHz, i.e., the antiferromagnetic resonance frequency.

4.3.1 Hard disk drive. The read/write heads of hard disk drives are another example of the application of ME effects [301]. A further increase in data record density implies a reduced bit size to the critical value of ~ 10 nm; smaller bits are likely to spontaneously remagnetize due to thermal fluctuations (the *superparamagnetic limit*). The superparamagnetic limit can be overcome by using media of large coercive force. Such media require high magnetic fields for recording information, which means an electric current step-up in the recording coils and, consequently, greater ohmic losses and losses through eddy currents.

Replacement of conventional inductive heads (Fig. 23a) by capacitance ME elements (Fig. 23b) would allow both the size of the write heads and the losses in them to be decreased. Application of a voltage to a capacitor in which the dielectric layer is composed of an ME material induces a magnetic field sufficient to provide individual data bit records (Fig. 23b).

The benefits of using electric fields for magnetic recording have already been demonstrated by a group of engineers affiliated with the Data Storage Institute, Singapore, based on commercial recording devices [302]. Specifically, the application of 3 V of voltage between the write head of the hard disk and its substrate allowed the write current to be decreased by 13%. The electric field causes a redistribution of electron density and, as a result, a decrease in magnetic

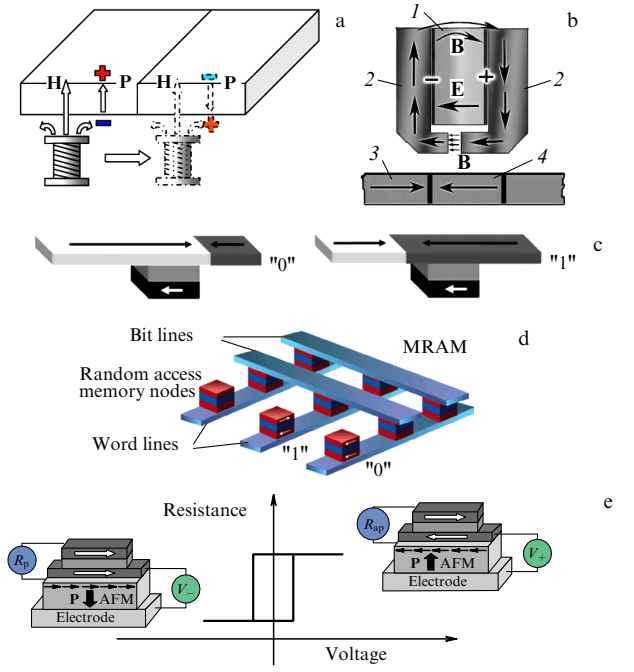

Figure 23. (a) Information readout from ME domains of opposite polarity. (b) Recording head based on a capacitive ME element [301]: *1* — ME layer between the plates across which an electric voltage is applied, *2* — magnetic conductor, *3* and *4* — domains with oppositely oriented magnetization corresponding to information bits 0 and 1. (c) The concept of the memory cell with a mobile domain boundary. Position of the domain wall in the free layer of a 'spin valve' type structure varies under the action of spin-polarized current pulses. Readout is based on the giant magnetoresistance effect [304]. (d) Schematic of magnetic random access memory with memory elements located at nodes [309]. (e) ME memory element (a heterostructure) in the '0' and '1' states (bottom and top, respectively). The heterostructure comprises a metallic electrode (lower layer), a layer of antiferromagnetic multiferroic (AFM), and a spin valve (two layers of magnetic conductors separated by a nonmagnetic spacer). The lower valve layer is exchange coupled to the multiferroic layer (see Ref. [179] for details).

anisotropy and the coercive field. Although the 'electric write/magnetic read' principle is only partly realized in such devices, it is worthy of attention as an alternative approach to overcoming the superparamagnetic limit, the development of which is currently underway. One of them is heat-assisted magnetic recording (HAMR) implying integration of miniature lasers into the write head.

4.3.2 Domain boundaries as memory devices. The most negative attribute of traditional magnetic storage devices, primarily hard disks, is their moving elements limiting the operation speed and strikingly increasing sensitivity to mechanical impacts; hence, an attractive idea to use in storage devices the movements and transformations of domain boundaries that are not accompanied by mechanical displacements of any element [303–306].

According to the modern racetrack memory concept being elaborated by Stewart Parkin [303], domain boundaries pass by the read head. Notches along the edges of the racetrack promote discrete transitions of domain boundaries from one stable position to another. A variant of this memory type is an element with two logical states (with high and low resistance) specified by the domain boundary position (Fig. 23c) [304]. It is planned to utilize pulses of spin-polarized current to both displace domain boundaries and record information. Nevertheless, with current density amounting to 10^6-10^7 A cm^{-2}, large power loss and degradation of elements can be anticipated.

In connection with this, those ME effects that allow changing the position of the domain boundary by an electric field either in media with a strong flexomagnetoelectric effect [iron garnet films [157, 158] (see Section 3.3)] or in composite structures constituted of a piezoelectric and a magnetic material whose domain structure is altered by a mechanical impact [307, 308], are of interest.

4.3.3 Magnetoelectric MRAM. Currently, various forms of *magnetoresistive random access memory* (MRAM) are being considered as a new generation of memories combining the high operation speed of semiconductor memory and the ability to store information in the absence of electric energy supply (nonvolatility), characteristic of magnetic memory [309] (Fig. 23d). MRAM nodes harbor tunneling contacts, i.e., structures operating on the basis of a giant magnetoresistance effect and combining both a recording medium (remagnetizable layer) and readout devices (the contact resistance of which depends on the degree of magnetization in the recording layer). Each memory element can be accessed by feeding read/write currents to the corresponding bit and number busses, with a given bit of information stored at their intersection. Bit magnetization is controlled by current signals; therefore, the problem of reducing energy losses remains to be resolved. Moreover, miniaturization brings to light the electromigration of metal ions in the course of passing a high-density current. These problems can be solved by means of recording information based on the ME effect [179, 221, 310, 311]. Because remagnetization in an ME element occurs under the action of a static electric field rather than current, additional energy loss can be avoided.

Figure 23e illustrates one of the realizations of a magnetic memory element [179] switched by an electric field and based on a heterostructure composed of a multiferroic and a 'spin valve' type multilayer structure used in the readout heads of modern hard discs [309]. The multiferroic layer is exchange coupled to the ferromagnetic conducting layer (a heterostructure on bismuth ferrite and $La_{0.7}Sr_{0.3}MnO_3$ [312]). Application of an electric voltage across the gate switches electric polarization of the multiferroic and induces reorganization of its antiferromagnetic structure (see Section 3.1) which, in turn, is converted to switching the magnetization of the adjacent magnetic layer. The net result is a change in relative orientation of magnetizations in the spin valve layers and a jumpwise variation of the electrical resistance of the structure (Fig. 23e).

The development of other scenarios for the employment of multiferroics in spin valves is currently underway, e.g. as dielectric spacers between two magnetic layers of the valve. In this case, the tunnel magnetoresistance of the structure will strongly depend on electric polarization [311, 313].

The use of semiconductors other than magnetic ferroelectrics and insulators for the creation of ME elements in spintronics is being considered. For example, the magnetic properties of Mn-doped gallium arsenide depend on the concentration of free charge carriers involved in exchange interactions between impurity Mn atoms. This enables control over magnetism in a semiconducting medium by applying voltage across the gate [314, 315].

Finally, composite-based elements in which changes in the magnetic state by applying voltage are mediated through mechanical strain offer ample possibilities for spintronic applications. It was estimated that ME composite-based elements necessitate hundreds of times less energy to be switched than modern transistors (a few hundred and even tens of k_BT [316–318]).

4.3.4 Spin field effect transistor. The key element of traditional microelectronics is the field effect transistor. The idea behind this device is to control electric currents by varying the gate voltage. The same principle underlies attempts to design spintronic devices in which magnetic moments of free electrons would be driven by electric potential.

The idea of a spin field effect transistor was suggested by S Datta and B Das in the paper "Electronic analog of the electrooptic modulator" from 1990 [319]. The self-explanatory title implies the use of spin-polarized electrons instead of polarized light. The spin field effect transistor has additional advantages over traditional field effect transistors. Specifically, it preserves its state even in the absence of an electric power supply, i.e. is nonvolatile and therefore may serve as a storage element [312, 320].

4.4 Microwave, magnonic, and magnetophotonic devices

The idea of control of magnetic resonance frequency underlies the application of ME materials in microwave devices. An ME material is placed in a permanent magnet field so that its antiferromagnetic resonance frequency is similar to the frequency of the microwave radiation being used. The applied voltage slightly changes the magnetic field in which the ME material is placed and thereby shifts the magnetic resonance frequency; this markedly alters absorption of microwave radiation power [49, 50]. Because magnetoelectrics constitute materials with time reversal violation, they can be used as nonreciprocal microwave devices, such as valves and circulators. Quadratic ME effects can be applied in frequency doubling devices [321, 322].

One more approach to the practical application of an additional degree of freedom (spin) is feasible, alongside the

exploitation of transport properties of spin-polarized electrons. It consists in using spin waves in logic spintronic devices. This research field is known as *magnonics*. Here, as in photonics, a high operation speed in the terahertz range can be achieved. The degree of compatibility between magnonics and spintronics is even higher than that between photonics and traditional electronics.

Unlike a spin-polarized current in which information about initial spin polarization is conserved during its propagation through a ferromagnet over a distance less than 1 μm, spin waves remain coherent at room temperature on a length scale up to 1 mm, making them attractive for application in spin computations. However, spin waves have a serious drawback: the amplitude of a wave traveling in a medium decreases exponentially with increasing distance due to magnon–phonon, magnon–magnon, and other forms of scattering. The most natural way to avoid this problem is to introduce additional elements, namely spin wave amplifiers, into integrated circuits. Such an amplifier based on the ME effect was proposed in Ref. [323]. Figure 24a shows a device in the form of a layered structure comprising a silicon substrate, a film of conducting ferromagnetic material through which spin waves propagate, and a piezoelectric layer with a metal gate. Electric potential applied to the gate causes mechanical stress in the piezoelectric layer, which is further transferred to the adjacent ferromagnetic layer. As a result, magnetostriction in the ferromagnetic layer causes the direction of the anisotropy axis to change by 90° (Fig. 24b).

Synchronous variations of gate voltage and spin wave oscillations allow the oscillation amplitude to be increased by several orders of magnitude (the process resembling parametric build-up of pendulum oscillations). Spin wave amplification in such a device increases the attenuation length up to hundreds of micrometers.

The discovery of electric field-excited magnonic modes (electromagnons) in ME materials [81] opened up new prospects for magnonics. Indeed, a method for electric guidance of spin waves was proposed, permitting us to avoid considerable energy loss inherent in former techniques (utilizing magnetic field or spin currents). The first encouraging results were obtained in bismuth ferrite studies; namely, the spin wave frequency shift under exposure to a 100-kV-cm^{-1} electric field at room temperature amounted to 30% [262].

Magnetoelectric materials can be applied to modulate radiation not only in microwave or terahertz frequency ranges but also in the optical one. The first reports describing electric field action on the magneto-optical rotation angle of the light polarization plane date back to the mid-1980s [85]. However, the so-called electromagneto-optical effect proved rather weak (not higher than a few dozen arcseconds for iron garnets in 10-kV cm^{-1} electric fields, in agreement with the relative change in the Faraday rotation angle equaling 0.01%) [273]. Because an electric field sets in motion the domain boundaries in iron garnet films (see Section 2.3), it can markedly change the Faraday rotation angle of a light beam focused onto the boundary (Fig. 24c). A sharp (more than 10-fold) enhancement of the electromagneto-optical effect at the domain boundaries was actually observed in Refs [324, 325]. However, the operation speed of devices based on the phenomenon of domain boundary motion does not exceed 1 GHz at the domain wall velocity of about 100 m s^{-1}.

An alternative approach in addressing this problem has its origin in the enhancement of magneto-optical effects in multilayer structures with refractive indices periodically varying on a wavelength scale (photonic crystals) [326–330]. A composite photonic crystal composed of magneto-optical and electro-optical layers exhibits an effective magneto-optical effect [331]. Another variant is a structure (Fig. 24d) in the form of a magnetic photonic crystal with a lattice into which a layer of nematic liquid crystal is introduced [332]. The low operation speed of such a system is compensated by the small driving voltage (from several tenths to tens of volts).

Finally, ME materials are expected to be employed to produce metamaterials and media with a negative refractive index (see relevant theoretical studies [333–336]).

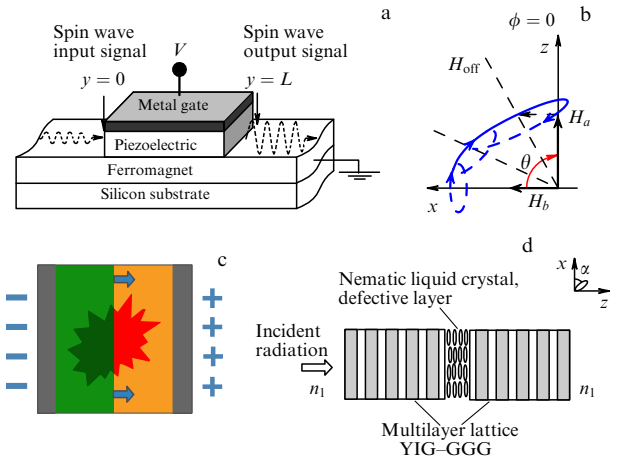

Figure 24. (a) Composite-based magnetoelectric element: mechanically coupled magnetostrictive material (e.g., CoFe or NiFe ferromagnet) and piezoelectric layer (e.g., lead zirconate titanate) [323]. (b) Parametric amplification in a spin wave upon a turn of the easy magnetization axis by 90°. (c) Electric field-induced motion of the domain boundary resulting in an intensity change in transmitted light focused on the domain boundary region. (d) Magnetic photonic crystal tuned by an electric field [332]. (YIG — yttrium iron garnet, and GGG — gadolinium gallium garnet.)

4.5 Wireless energy transfer and energy-saving technologies

The miniaturization of electronic devices brought about new technologies of wireless sensor networks incorporating a large number of sensors collecting, processing, and exchanging information. Such distributed self-organizing systems may be highly efficacious for monitoring the operational status of mechanisms, environmental conditions, and safety systems including those designed to avert terroristic threats.

The development of wireless sensor networks is restricted mostly by power supply problems. They become especially challenging when sensors need to be inserted inside study objects (e.g., to measure tire pressure in a moving vehicle) or cannot be connected to an electric power network. The most common way to resolve the power supply problem is to use electrochemical batteries. However, miniature high-capacity power sources evolve at a slower pace than solid-state electronics. Inasmuch as many wireless sensor networks are being designed for long-term exploitation, other solutions are needed.

The most attractive of them is so-called energy harvesting from external sources using systems accumulating the energy of mechanical, thermal, or electromagnetic oscillations. However, the energy flux derived from natural sources is too

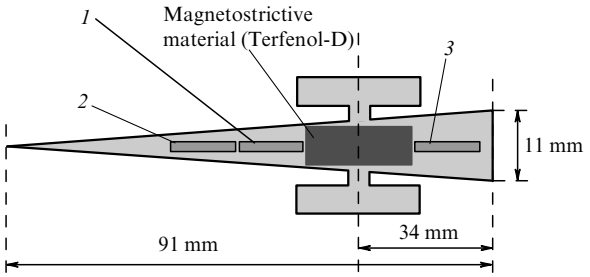

Figure 25. Magnetoelectric transformer made up of piezoelectric and magnetostrictive materials deposited onto a tapered metal substrate (waveguide acoustic concentrator); *1–3* — piezoelectric wafers [337].

small — less than 1 μW cm^{-2} (here, light emission is not referred to, because the sensors are not infrequently shielded from daylight, as noted before). For this reason, a special source of an alternating field powerful enough to ensure wireless energy feeding to many remote sensors is needed when designing sensor networks.

An ME device proposed in Ref. [337] accumulates energy from an alternating magnetic field for a rather long time (over 10 min), converts it into the energy of a capacitor bank, and eventually releases it in the form of a roughly 1-s-long electric pulse. The energy source is a power generator buried underground with an antenna that creates an alternating magnetic field with an amplitude of 1 Oe and a frequency of 30 kHz in the sensor location area. The energy of the magnetic field is converted into the electrostatic energy of charged capacitors by an ME element in the form of a plate with a tapered free end and a coat of magnetostrictive and piezoelectric layers over a common metal substrate (Fig. 25). The alternating magnetic field causes periodic deformation of the magnetostrictive layer at the resonance frequency. These mechanical oscillations are transmitted to the substrate and spread over it. As a result, acoustic energy concentration and oscillation amplitude increase toward the narrow end. Vibrations of the piezoelectric layers, transmitted from the vibrating substrate, give rise to an alternating voltage. This device is a variant of a magnetoelectric composite material. However, its ME coefficient is twice that of a traditional multilayer structure of magnetic and electric layers due to the presence of the acoustic concentrator. The ME transducer described in Ref. [337] may deliver the power supply of a sensor transmitting information over a distance of 60–100 m.

Mechanical motion or vibrations provide one more energy source more suitable for power supply to medical implants, autonomous sensors, communication facilities and mobile electronic devices. One of the most popular energy harvesting schemes takes advantage of a spring cantilever beam from a piezoelectric material (e.g., bismuth ferrite [219]) whose mechanical vibrations are converted into voltage oscillations. Calculations show that the efficiency of such a transformer can be significantly improved by utilizing thin (a few dozen nanometers) plates which admit the contribution from the flexoelectric effect. Indeed, flexural strain in the plate makes an additional contribution to polarization, which is greater by several-fold than that from the usual 'bulk' piezoelectric effect [338].

Further development of the above energy harvesting scheme with the use of ME materials was proposed in Ref. [339]. When the cantilever from a composite material (rigidly fastened piezoelectric and magnetostrictive layers) oscillates in Earth's magnetic field, the latter layer undergoes additional strain. Its transmission to the piezoelectric layer doubles the alternating voltage amplitude to several dozen volts, as opposed to that in a purely piezoelectric cantilever. The authors of Ref. [339] propose installing such devices in underwater equipment and buoys to take advantage of the energy of sea waves and Earth's magnetic field.

It should be emphasized that oscillation frequencies ω are not high under natural conditions (a few hertz or tens of hertz at the most). This means, first, that the power generated by a given device is small (proportional to the product of the inertial force and velocity amplitudes, i.e. the cube of the frequency) and, second, that the size of the device (for which such frequencies are actually eigenfrequencies) is far from being microscopic [340]. The system described in Ref. [339] is constructed as a plate (length 10 cm, width 2 cm, thickness 3 mm) with a load of 1 g and specific power of 1 μW cm^{-3} (for comparison, a lithium-ion battery of 1 kJ cm^{-3} capacity can operate in such a mode for 30 years). Better results are expected from the exploitation of other forms of vibrational motion, such as the whole-body vibrations of a person walking (piezoelectric elements implanted in the shoe soles already produce up to 1 mW cm^{-3}) and even higher-frequency vibrations of a car engine (up to 30 mW cm^{-3}). However, it is premature to speak of substituting such elements for the batteries in mobile phones and portable computers, because the needed energy has to be gleaned from different sources; hence, the term 'energy scavenging' is a close synonym of 'energy harvesting'.

5. Conclusion

It is appropriate to emphasize once again that all the practical implementations cited in this review (except, possibly, magnetic field sensors) are just ideas or laboratory prototypes. The prospects of practical realization of devices based on magnetoelectrics and multiferroics was and remains a powerful impetus for developments in this field of solid-state physics and nanotechnology. Extensive studies over the last decade have contributed greatly to our understanding of magnetoelectric interactions and the mechanisms of electric polarization emergence. Also, multiferroics served as a touchstone in the development of methods for numerical calculations of crystals. In conclusion, the nascent field of solid-state physics outlined in this report is still in its infancy, some of its concepts await further elaboration, and most practical implementations have yet to be fully realized.

Acknowledgments

The authors wish to express their appreciation to A M Kadomtseva and A P Levanyuk for reading the manuscript, taking an interest in this work, and providing valuable comments. We gratefully acknowledge the collaboration and discussions with V G Bar'yakhtar, V N Berzhansky, Manuel Bibes, M I Bichurin, A A Bush, D Viehland, Michel Viret, G P Vorob'ev, Z V Gareeva, L P Gorkov, K A Zvezdin, S A Zvyagin, G A Meshkov, V Yu Ivanov, M D Kuz'min, Yu V Kopaev, Jiefang Li, F V Lisovskii, I S Lyubutin, A I Morozov, Wolfgang Kleemann, S S Krotov, M V Mostovoy, A A Mukhin, A V Nikolaev, E P Nikolaeva, N S Perov, R V Pisarev, Yu F Popov, A I Popov, A S Sergeev, D A Sechin, A S Sigov, James F Scott, Sh-J Sun, M P Temiryazeva, Masashi Tokunaga, Yu K Fetisov, D A Filippov,

A M Hagiri-Gosnet, D I Khomsky, Hsiung Chou, and Hans Schmid. Our special thanks go to Z A Pyatakova for her contributions to the design of pictures.

The work was supported by RFBR grants Nos 11-02-12170-ofi-m and 10-02-13302-RT_omi.

References

1. Hill N A *J. Phys. Chem. B* **104** 6694 (2000)
2. Fiebig M et al. *Nature* **419** 818 (2002)
3. Schmid H "Magnetoelectric effects in insulating magnetic materials", in *Introduction to Complex Mediums for Optics and Electromagnetics* (Eds W S Weiglhofer, A Lakhtakia) (Bellingham, WA: SPIE Optical Engineering Press, 2003) p. 167
4. Zvezdin A K, Pyatakov A P *Usp. Fiz. Nauk* **174** 465 (2004) [*Phys. Usp.* **47** 416 (2004)]
5. Fiebig M *J. Phys. D Appl. Phys.* **38** R123 (2005)
6. Eerenstein W, Mathur N D, Scott J F *Nature* **442** 759 (2006)
7. Cheong S-W, Mostovoy M *Nature Mater.* **6** 13 (2007)
8. Wang K F, Liu J-M, Ren Z F *Adv. Phys.* **58** 321 (2009)
9. Picozzi S, Ederer C *J. Phys. Condens. Matter* **21** 303201 (2009)
10. Zvezdin A K, Pyatakov A P *Usp. Fiz. Nauk* **179** 897 (2009) [*Phys. Usp.* **52** 845 (2009)]
11. Khomskii D *Physics* **2** 20 (2009)
12. Chupis I E *Fiz. Nizk. Temp.* **36** 597 (2010) [*Low Temp. Phys.* **36** 477 (2010)]
13. Chupis I E, arXiv:1012.2024
14. Scott J F, Blinc R *J. Phys. Condens. Matter* **23** 113202 (2011)
15. Smolenskii G A, Chupis I E *Usp. Fiz. Nauk* **137** 415 (1982) [*Sov. Phys. Usp.* **25** 475 (1982)]
16. O'Dell T H *Electron. Power* **11** 266 (1965)
17. O'Dell T H *The Electrodynamics of Magneto-Electric Media* (Amsterdam: North-Holland, 1970)
18. Freeman A J, Schmid H (Eds) *Magnetoelectric Interaction Phenomena in Crystals* (London: Gordon and Breach Sci. Publ., 1975)
19. Venevtsev Yu N, Gagulin V V, Lyubimov V N *Segnetomagnetiki* (Seignetomagnetics) (Moscow: Nauka, 1982)
20. Curie P *J. Physique III* 393 (1894)
21. Boguslavskii S A *Izbrannye Trudy po Fizike* (Selected Works on Physics) (Moscow: Fizmatgiz, 1961)
22. Debye P *Z. Phys.* **35** 300 (1926)
23. Tellegen B D H *Philips Res. Rep.* **3** 81 (1948)
24. Landau L D, Lifshitz E M *Elektrodinamika Sploshnykh Sred* (Electrodynamics of Continuous Media) (Moscow: Nauka, 1992) p. 266 [Translated into English (Oxford: Pergamon Press, 1984)]
25. Dzyaloshinskii I E *Zh. Eksp. Teor. Fiz.* **37** 881 (1959) [*Sov. Phys. JETP* **10** 628 (1960)]
26. Astrov D N *Zh. Eksp. Teor. Fiz.* **38** 984 (1960) [*Sov. Phys. JETP* **11** 708 (1960)]
27. Folen V J, Rado G T, Stalder E W *Phys. Rev. Lett.* **6** 607 (1961)
28. Popov Yu F, Kazei Z A, Kadomtseva A M *Pis'ma Zh. Eksp. Teor. Fiz.* **55** 238 (1992) [*JETP Lett.* **55** 234 (1992)]
29. Belov D V et al. *Pis'ma Zh. Eksp. Teor. Fiz.* **58** 603 (1993) [*JETP Lett.* **58** 579 (1993)]
30. Turov E A *Usp. Fiz. Nauk* **164** 325 (1994) [*Phys. Usp.* **37** 303 (1994)]
31. Turov E A et al. *Simmetriya i Fizicheskie Svoistva Antiferromagnetikov* (Symmetry and Physical Properties of Antiferromagnets) (Moscow: Fizmatlit, 2001) p. 239
32. Dubovik V M, Tugushev V V *Phys. Rep.* **187** 145 (1990)
33. Ginzburg V L et al. *Solid State Commun.* **50** 339 (1984)
34. Sannikov D G, Zheludev I S *Fiz. Tverd. Tela* **27** 1369 (1985) [*Sov. Phys. Solid State* **27** 826 (1985)]
35. Schmid H *Ferroelectrics* **252** 41 (2001)
36. Popov Yu F et al. *Zh. Eksp. Teor. Fiz.* **114** 263 (1998) [*JETP* **87** 146 (1998)]
37. Kopaev Yu V *Usp. Fiz. Nauk* **179** 1175 (2009) [*Phys. Usp.* **52** 1111 (2009)]
38. Gorbatsevich A A, Omel'yanovskii O E, Tsebro V I *Usp. Fiz. Nauk* **179** 887 (2009) [*Phys. Usp.* **52** 835 (2009)]
39. Popov Yu F et al. *Pis'ma Zh. Eksp. Teor. Fiz.* **69** 302 (1999) [*JETP Lett.* **69** 330 (1999)]
40. Krotov S S et al. *J. Magn. Magn. Mater.* **226–230** 963 (2001)
41. Tagantsev A K *Usp. Fiz. Nauk* **152** 423 (1987) [*Sov. Phys. Usp.* **30** 588 (1987)]
42. Strukov B A, Levanyuk A P *Fizicheskie Osnovy Segnetoelektricheskikh Yavlenii v Kristallakh* (Ferroelectric Phenomena in Crystals: Physical Foundations) (Moscow: Nauka, 1983) [Translated into English (Berlin: Springer, 1998)]
43. Ederer C, Spaldin N *Phys. Rev. B* **76** 214404 (2007)
44. Spaldin N A, Fiebig M, Mostovoy M *J. Phys. Condens. Matter* **20** 434203 (2008)
45. Popov A I, Plokhov D I, Zvezdin A K *Europhys. Lett.* **87** 67004 (2009)
46. Plokhov D I, Zvezdin A K, Popov A I *Phys. Rev. B* **83** 184415 (2011)
47. Rado G T, Ferrari J M, Maisch W G *Phys. Rev. B* **29** 4041 (1984)
48. Nénert G, Palstra T T M *Phys. Rev. B* **76** 024415 (2007)
49. Bichurin M I et al. *Magnitoelektricheskii Effekt v Kompozitsionnykh Materialakh* (Magnetoelectric Effect in Composite Materials) (Velikii Novgorod: Novgor. Gos. Univ., 2005)
50. Fetisov Y K, Srinivasan G *Appl. Phys. Lett.* **88** 143503 (2006)
51. Fetisov Y K et al. *IEEE Sensor J.* **6** 935 (2006)
52. Nan C-W et al. *J. Appl. Phys.* **103** 031101 (2008)
53. Jing Ma et al. *Adv. Mater.* **23** 1062 (2011)
54. Smolenskii G A et al. *Izv. Akad. Nauk SSSR Ser. Fiz.* **25** 1333 (1961)
55. Schmid H *Ferroelectrics* **162** 317 (1994)
56. Popov Yu F et al. *Zh. Eksp. Teor. Fiz.* **138** 226 (2010) [*JETP* **111** 199 (2010)]
57. Kadomtseva A M et al. *Fiz. Nizk. Temp.* **36** 640 (2010) [*Low Temp. Phys.* **36** 511 (2010)]
58. Choi Y J et al. *Phys. Rev. Lett.* **105** 097201 (2010)
59. Golovenchits E I, Sanina V A *Pis'ma Zh. Eksp. Teor. Fiz.* **84** 222 (2006) [*JETP Lett.* **84** 190 (2006)]
60. Gufan Yu M *Pis'ma Zh. Eksp. Teor. Fiz.* **8** 271 (1968) [*JETP Lett.* **8** 167 (1968)]
61. Levitin R Z et al. *Pis'ma Zh. Eksp. Teor. Fiz.* **79** 531 (2004) [*JETP Lett.* **79** 423 (2004)]
62. Pankrats A I et al. *Zh. Eksp. Teor. Fiz.* **126** 887 (2004) [*JETP* **99** 766 (2004)]
63. Chukalina E P et al. *Phys. Lett. A* **322** 239 (2004)
64. Zvezdin A K et al. *Pis'ma Zh. Eksp. Teor. Fiz.* **81** 335 (2005) [*JETP Lett.* **81** 272 (2005)]
65. Kharlamova S A et al. *Zh. Eksp. Teor. Fiz.* **128** 1252 (2005) [*JETP* **101** 1098 (2005)]
66. Zvezdin A K et al. *Pis'ma Zh. Eksp. Teor. Fiz.* **83** 600 (2006) [*JETP Lett.* **83** 509 (2006)]
67. Vasiliev A N, Popova E A *Fiz. Nizk. Temp.* **32** 968 (2006) [*Low Temp. Phys.* **32** 735 (2006)]
68. Popova M N *J. Magn. Magn. Mater.* **321** 716 (2009)
69. Popova E A et al. *Phys. Rev. B* **75** 224413 (2007)
70. Kadomtseva A M et al. *Fiz. Nizk. Temp.* **32** 933 (2006) [*Low Temp. Phys.* **32** 709 (2006)]
71. Harris A B et al. *Phys. Rev. B* **78** 014407 (2008)
72. Harris A B, Aharony A, Entin-Wohlman O *J. Phys. Condens. Matter* **20** 434202 (2008)
73. Moskvin A S, Drechsler S-L *Eur. Phys. J.* **71** 331 (2009)
74. Krotov S S, Shnaidshtein I V *Fenomenologiya Magnitoindutsirovannogo Segnetoelektrichestva* (Phenomenology of Magnetoinduced Ferroelectricity) (Moscow: Fiz. Fakul'tet MGU, 2011)
75. Sadykov A F et al. *Pis'ma Zh. Eksp. Teor. Fiz.* **92** 580 (2010) [*JETP Lett.* **92** 527 (2010)]
76. Baturov L N, Al'shin B I, Yarmukhamedov Yu N *Fiz. Tverd. Tela* **20** 2254 (1978) [*Sov. Phys. Solid State* **20** 1300 (1978)]
77. Goto T et al. *Phys. Rev. Lett.* **92** 257201 (2004)
78. Mukhin A A et al. *Pis'ma Zh. Eksp. Teor. Fiz.* **93** 305 (2011) [*JETP Lett.* **93** 275 (2011)]
79. Smirnov A I, Khlyustikov I N *Usp. Fiz. Nauk* **165** 1215 (1995) [*Phys. Usp.* **38** 1169 (1995)]
80. Turov E A, Nikolaev V V *Usp. Fiz. Nauk* **175** 457 (2005) [*Phys. Usp.* **48** 431 (2005)]
81. Pimenov A et al. *Nature Phys.* **2** 97 (2006)
82. Mukhin A A et al. *Usp. Fiz. Nauk* **179** 904 (2009) [*Phys. Usp.* **52** 851 (2009)]
83. Sushkov A B et al. *J. Phys. Condens. Matter* **20** 434210 (2008)
84. Mochizuki M, Nagaosa N *Phys. Rev. Lett.* **105** 147202 (2010)

85. Krichevtsov B B, Pisarev R V, Selitskii A G *Pis'ma Zh. Eksp. Teor. Fiz.* **41** 259 (1985) [*JETP Lett.* **41** 317 (1985)]
86. Krichevtsov B B, Pavlov V V, Pisarev R V *Pis'ma Zh. Eksp. Teor. Fiz.* **44** 471 (1986) [*JETP Lett.* **44** 608 (1986)]
87. Pisarev R V et al. *J. Magn. Soc. Jpn.* **11** (S1) 33 (1987)
88. Saito M et al. *Nature Mater.* **8** 634 (2009)
89. Jung J H et al. *Phys. Rev. Lett.* **93** 037403 (2004)
90. Kida N et al. *Phys. Rev. Lett.* **94** 077205 (2005)
91. Agal'tsov A M et al. *Kratk. Soobshch. Fiz. FIAN* (5) 37 (1989) [*Sov. Phys. Lebedev Inst. Rep.* (5) 48 (1989)]
92. Aktsipetrov O A, Braginskii O V, Esikov D A *Kvantovaya Elektron.* **17** 320 (1990) [*Sov. J. Quantum Electron.* **20** 259 (1990)]
93. Pavlov V V et al. *Phys. Rev. Lett.* **78** 2004 (1997)
94. Kartavtseva M S et al. *Thin Solid Films* **515** 6416 (2007)
95. Aktsipetrov O A *J. Opt. Soc. Am. B* **28** (12) A27 (2011)
96. Ramirez M O et al. *Phys. Rev. B* **79** 224106 (2009)
97. Fröhlich D et al. *Phys. Rev. Lett.* **81** 3239 (1998)
98. Goltsev A V et al. *Phys. Rev. Lett.* **90** 177204 (2003)
99. Kartavtseva M S et al. *J. Mater. Res.* **22** 2063 (2007)
100. Meier D et al. *Phys. Rev. Lett.* **102** 107202 (2009)
101. Lee J H et al. *Nature* **466** 954 (2010)
102. Meier D et al. *Phys. Rev. B* **82** 155112 (2010)
103. Matsuura H et al. *Ferroelectrics* **410** 59 (2011)
104. Fiebig M et al. *Appl. Phys. Lett.* **66** 2906 (1995)
105. Van Aken B B et al. *Nature* **449** 702 (2007)
106. Bar'yakhtar V G, L'vov V A, Yablonskii D A *Pis'ma Zh. Eksp. Teor. Fiz.* **37** 565 (1983) [*JETP Lett.* **37** 673 (1983)]
107. Eliseev E A et al. *Phys. Rev. B* **84** 174112 (2011)
108. Sparavigna A, Strigazzi A, Zvezdin A *Phys. Rev. B* **50** 2953 (1994)
109. Dzyaloshinskii I *Europhys. Lett.* **83** 67001 (2008)
110. Pyatakov A P, Zvezdin A K *Eur. Phys. J. B* **71** 419 (2009)
111. Tanygin B M *J. Magn. Magn. Mater.* **323** 1899 (2011)
112. Mostovoy M *Phys. Rev. Lett.* **96** 067601 (2006)
113. Men'shenin V V *Zh. Eksp. Teor. Fiz.* **135** 265 (2009) [*JETP* **108** 236 (2009)]
114. Popov Yu F, Kadomtseva A M, Vorob'ev G P, Zvezdin A K *Ferroelectrics* **162** 135 (1994)
115. Kimura T et al. *Nature* **426** 55 (2003)
116. Kagawa F et al. *Phys. Rev. Lett.* **102** 057604 (2009)
117. Milov E V et al. *Pis'ma Zh. Eksp. Teor. Fiz.* **85** 610 (2007) [*JETP Lett.* **85** 503 (2007)]
118. Yamasaki Y et al. *Phys. Rev. Lett.* **98** 147204 (2007)
119. Newnham R E et al. *J. Appl. Phys.* **49** 6088 (1978)
120. Sosnowska I, Zvezdin A *J. Magn. Magn. Mater.* **140–144** 167 (1995)
121. Kimura T *Annu. Rev. Mater. Res.* **37** 387 (2007)
122. Tokura Y, Seki S *Adv. Mater.* **22** 1554 (2010)
123. Ishiwata Sh et al. *Science* **319** 1643 (2008)
124. Kitagawa Y et al. *Nature Mater.* **9** 797 (2010)
125. Soda M et al. *Phys. Rev. Lett.* **106** 087201 (2011)
126. Arima T *J. Phys. Soc. Jpn.* **76** 073702 (2007)
127. Nakajima T et al. *J. Phys. Soc. Jpn.* **76** 043709 (2007)
128. Frontzek M et al. *Phys. Rev. B* **84** 094448 (2011)
129. Johnson R D et al. *Phys. Rev. Lett.* **108** 067201 (2012)
130. Gehring G A *Ferroelectrics* **161** 275 (1994)
131. Rado G T *Phys. Rev. Lett.* **6** 609 (1961)
132. Date M, Kanamori J, Tachiki M *J. Phys. Soc. Jpn.* **16** 2589 (1961)
133. Hornreich R M, Shtrikman S *Phys. Rev.* **161** 506 (1967)
134. Sergienko I A, Dagotto E *Phys. Rev. B* **73** 094434 (2006)
135. Keffer F, Moriya T *Phys. Rev.* **126** 896 (1962)
136. Moskvin A S, Bogstrem I G *Fiz. Tverd. Tela* **19** 1616 (1977) [*Sov. Phys. Solid State* **19** 1532 (1977)]
137. van den Brink J, Khomskii D I *J. Phys. Condens. Matter* **20** 434217 (2008)
138. Walker H C et al. *Science* **333** 1273 (2011)
139. Rondinelli J M, Stengel M, Spaldin N A *Nature Nanotechnol.* **3** 46 (2008)
140. Valencia S et al. *Nature Mater.* **10** 753 (2011)
141. Duan C-G, Jaswal S S, Tsymbal E Y *Phys. Rev. Lett.* **97** 047201 (2006)
142. Meyerheim H L et al. *Phys. Rev. Lett.* **106** 087203 (2011)
143. Moore J E *Nature* **464** 194 (2010)
144. Kopaev Yu V, Gorbatsevich A A, Belyavskii V I *Kristallografiya* **56** 906 (2011) [*Crystallogr. Rep.* **56** 848 (2011)]
145. Qi X-L, Hughes T L, Zhang S-C *Phys. Rev. B* **78** 195424 (2008)
146. Wilczek F *Phys. Rev. Lett.* **58** 1799 (1987)
147. Singh M P et al. *Phase Transit.* **79** 973 (2006)
148. Ogawa Y et al. *Phys. Rev. Lett.* **90** 217403 (2003)
149. Geprags S et al. *Philos. Mag. Lett.* **87** 141 (2007)
150. Krockenberger Y et al. *Phys. Rev. B* **83** 214414 (2011)
151. Zvezdin A K *Kratk. Soobshch. Fiz. FIAN* **7** (4) 5 (2002) [*Bull. Lebedev Physics Inst.* (4) 7 (2002)]
152. Bode M et al. *Nature* **447** 190 (2007)
153. Serrate D et al. *Nature Nanotechnol.* **5** 350 (2010)
154. Heide M, Bihlmayer G, Blügel S *Phys. Rev. B* **78** 140403(R) (2008)
155. Pyatakov A P et al. *Europhys. Lett.* **93** 17001 (2011)
156. Catalan G et al. *Rev. Mod. Phys.* **84** 119 (2012)
157. Logginov A S, Meshkov G A, Nikolaev A V, Pyatakov A P *Pis'ma Zh. Eksp. Teor. Fiz.* **86** 124 (2007) [*JETP Lett.* **86** 115 (2007)]
158. Logginov A S et al. *Appl. Phys. Lett.* **93** 182510 (2008)
159. Gareeva Z V, Zvezdin A K *Phys. Status Solidi RRL* **3** 79 (2009)
160. Gareeva Z V, Zvezdin A K *Europhys. Lett.* **91** 47006 (2010)
161. Gareeva Z V, Zvezdin A K *Fiz. Tverd. Tela* **52** 1595 (2010) [*Phys. Solid State* **52** 1714 (2010)]
162. Lubk A, Gemming S, Spaldin N A *Phys. Rev. B* **80** 104110 (2009)
163. Daraktchiev M, Catalan G, Scott J F *Phys. Rev. B* **81** 224118 (2010)
164. Seidel J et al. *Nature Mater.* **8** 229 (2009)
165. Maksymovych P et al. *Nano Lett.* **11** 1906 (2011)
166. Béa H, Paruch P *Nature Mater.* **8** 168 (2009)
167. Smolenskii G A (Ed.) *Fizika Magnitnykh Dielektrikov* (Physics of Magnetic Dielectrics) (Leningrad: Nauka, 1974)
168. Royen P, Swars K *Angew. Chem.* **69** 779 (1957)
169. Teague J R, Gerson R, James W J *Solid State Commun.* **8** 1073 (1970)
170. Fischer P, Polomska M *J. Phys. C Solid State* **13** 1931(1980)
171. Kadomtseva A M et al. *Pis'ma Zh. Eksp. Teor. Fiz.* **79** 705 (2004) [*JETP Lett.* **79** 571 (2004)]
172. Kadomtseva A M et al. *Phase Transit.* **79** 1019 (2006)
173. Catalan G, Scott J F *Adv. Mater.* **21** 2463 (2009)
174. Lane W M *Appl. Phys. Lett.* **97** 173105 (2010)
175. Kalinkin A N, Skorikov V M *Zh. Neorgan. Khim.* **55** 1903 (2010) [*Russ. J. Inorganic Chem.* **97** 1794 (2010)]
176. Logginov A S, Pyatakov A P, Zvezdin A K *Proc. SPIE* **5955** 56 (2005)
177. Béa H et al. *Appl. Phys. Lett.* **88** 062502 (2006)
178. Zvezdin A K, Logginov A S, Meshkov G A, Pyatakov A P *Izv. Ross. Akad. Nauk Ser. Fiz.* **71** 1604 (2007) [*Bull. Russ. Acad. Sci. Phys.* **71** 1561 (2007)]
179. Bibes M, Barthélémy A *Nature Mater.* **7** 425 (2008)
180. Alexe M, Hesse D *Nature Commun.* **2** 256 (2011)
181. Kehr S C et al. *Nature Commun.* **2** 249 (2011)
182. Wang X et al. *J. Alloys Compounds* **509** 6585 (2011)
183. Dai Z, Fujita Y, Akishige Y *Mater. Lett.* **65** 2036 (2011)
184. Zinenko V I, Pavlovskii M S *Pis'ma Zh. Eksp. Teor. Fiz.* **87** 338 (2008) [*JETP Lett.* **87** 288 (2008)]
185. Zinenko V I, Pavlovskii M S *Fiz. Tverd. Tela* **51** 1328 (2009) [*Phys. Solid State* **51** 1404 (2009)]
186. Plakhtii V P, Mal'tsev E I, Kaminker D M *Izv. Akad. Nauk SSSR Ser. Fiz.* **28** 436 (1963)
187. Kubel B F, Schmid H *Acta Cryst. B* **46** 698 (1990)
188. Thomas H, Muller K A *Phys. Rev. Lett.* **21** 1256 (1968)
189. Gabbasova Z V et al. *Phys. Lett. A* **158** 491 (1991)
190. Moreau J M et al. *J. Phys. Chem. Solids* **32** 1315 (1971)
191. Wang J et al. *Science* **299** 1719 (2003)
192. Li J et al. *Appl. Phys. Lett.* **84** 5261 (2004)
193. Lebeugle D et al. *Phys. Rev. B* **76** 024116 (2007)
194. Eerenstein W et al. *Science* **307** 1203 (2005)
195. Neaton J B et al. *Phys. Rev. B* **71** 014113 (2005)
196. Mukhortov V M, Golovko Yu I, Yuzyuk Yu I *Usp. Fiz. Nauk* **179** 909 (2009) [*Phys. Usp.* **52** 856 (2009)]
197. Yun K Y et al. *Jpn. J. Appl. Phys.* **43** L647 (2004)
198. Maruyama K et al. *FUJITSU Sci. Tech. J.* **43** (4) 502 (2007)
199. Ederer C, Spaldin N A *Phys. Rev. B* **71** 060401(R) (2005)
200. Tabares-Munoz C et al. *Jpn. J. Appl. Phys.* **24** (Suppl. 24-2) 1051 (1985)

201. Sosnowska I, Peterlin-Neumaier T, Steichele E *J. Phys. C* **15** 4835 (1982)
202. Zvezdin A K, Pyatakov A P *Phys. Status Solidi B* **246** 1956 (2009)
203. Ramazanoglu M et al. *Phys. Rev. Lett.* **107** 207206 (2011)
204. Zalesskii A V, Zvezdin A K, Frolov A A, Bush A A *Pis'ma Zh. Eksp. Teor. Fiz.* **71** 682 (2000) [*JETP Lett.* **71** 465 (2000)]
205. Zalesskii A V et al. *Fiz. Tverd. Tela* **45** (1) 134 (2003) [*Phys. Solid State* **45** 141 (2003)]
206. Zhdanov A G et al. *Fiz. Tverd. Tela* **48** (1) 83 (2006) [*Phys. Solid State* **48** 88 (2006)]
207. Pokatilov V S, Sigov A S *Zh. Eksp. Teor. Fiz.* **137** 498 (2010) [*JETP* **110** 440 (2010)]
208. Ramazanoglu M et al. *Phys. Rev. B* **83** 174434 (2011)
209. Sosnowska I, Przeniosło R *Phys. Rev. B* **84** 144404 (2011)
210. Kulagin N E, Popkov A F, Zvezdin A K *Fiz. Tverd. Tela* **53** 912 (2011) [*Phys. Solid State* **53** 970 (2011)]
211. Popov Yu F et al. *Pis'ma Zh. Eksp. Teor. Fiz.* **57** 65 (1993) [*JETP Lett.* **57** 69 (1993)]
212. Tehranchi M M, Kubrakov N F, Zvezdin A K *Ferroelectrics* **204** 181 (1997)
213. Tokunaga M, Azuma M, Shimakawa Y *J. Phys. Soc. Jpn.* **79** 064713 (2010)
214. Yun K Y, Noda M, Okuyama M *Appl. Phys. Lett.* **83** 3981 (2003)
215. Bai F et al. *Appl. Phys. Lett.* **86** 032511 (2005)
216. Béa H et al. *Appl. Phys. Lett.* **87** 072508 (2005)
217. Ramesh R, Spaldin N A *Nature Mater.* **6** 21 (2007)
218. Kumar A, Scott J F, Katiyar R S *Appl. Phys. Lett.* **99** 062504 (2011)
219. Prashanthi K et al. *Sensors Actuators A* **166** 83 (2011)
220. Wojdel J C, Iniguez J *Phys. Rev. Lett.* **105** 037208 (2010)
221. Zhao T et al. *Nature Mater.* **5** 823 (2006)
222. Borisov P et al. *Phys. Rev. Lett.* **94** 117203 (2005)
223. Borisov P et al. *Phase Transit.* **79** 1123 (2006)
224. Laukhin V et al. *Phys. Rev. Lett.* **97** 227201 (2006)
225. Chu Y-H et al. *Nature Mater.* **7** 478 (2008)
226. Heron J T et al. *Phys. Rev. Lett.* **107** 217202 (2011)
227. Palkar V R, Prashanthi K *Appl. Phys. Lett.* **93** 132906 (2008)
228. Wang J et al. *Appl. Phys. Lett.* **85** 2574 (2004)
229. Wang D H et al. *Appl. Phys. Lett.* **89** 182905 (2006)
230. Wang Y, Nan C-W *Thin Solid Films* **517** 4484 (2009)
231. Ramazanoglu M et al. *Phys. Rev. Lett.* **107** 067203 (2011)
232. Haumont R et al. *Phys. Rev. B* **79** 184110 (2009)
233. Gavriliuk A G et al. *Pis'ma Zh. Eksp. Teor. Fiz.* **82** 243 (2005) [*JETP Lett.* **82** 224 (2008)]
234. Gavriliuk A G et al. *Phys. Rev. B* **77** 155112 (2008)
235. Lyubutin I S, Gavrilyuk A G, Struzhkin V V *Pis'ma Zh. Eksp. Teor. Fiz.* **88** 601 (2008) [*JETP Lett.* **88** 524 (2008)]
236. Murashev V A et al. *Kristallografiya* **35** 912 (1990) [*Sov. Phys. Crystallogr.* **35** 538 (1990)]
237. Kadomtseva A M et al. *Ferroelectrics* **169** 85 (1995)
238. Khomchenko V A et al. *J. Appl. Phys.* **108** 074109 (2010)
239. Vorob'ev G P et al. *Fiz. Tverd. Tela* **37** 2428 (1995) [*Phys. Solid State* **37** 1329 (1995)]
240. Troyanchuk I O et al. *Pis'ma Zh. Eksp. Teor. Fiz.* **89** 204 (2009) [*JETP Lett.* **89** 180 (2009)]
241. Pokatilov V S, Sigov A S, Konovalova A O *Pis'ma Zh. Eksp. Teor. Fiz.* **94** 757 (2011) [*JETP Lett.* **94** 698 (2011)]
242. Wang N et al. *Phys. Rev. B* **72** 104434 (2005)
243. Troyanchuk I O et al. *Pis'ma Zh. Eksp. Teor. Fiz.* **93** 570 (2011) [*JETP Lett.* **93** 512 (2011)]
244. Yuan G L, Siu Wing Or *Appl. Phys. Lett.* **88** 062905 (2006)
245. Kuznetsov M A et al. *Nano- i Mikrosistemnaya Tekh.* (12) 20 (2007)
246. Reznichenko L A et al. *Kratk. Soobshch. Fiz. FIAN* (1) 27 (2010) [*Bull. Lebedev Phys. Inst.* **37** (1) 16 (2010)]
247. Fujino S et al. *Appl. Phys. Lett.* **92** 202904 (2008)
248. Palkar V R et al. *Appl. Phys. Lett.* **84** (15) 2856 (2004)
249. Qi X et al. *Appl. Phys. Lett.* **86** 062903 (2005)
250. Zhang X Y et al. *Appl. Phys. Lett.* **87** 143102 (2005)
251. Murakami M et al. *Appl. Phys. Lett.* **88** 112505 (2006)
252. Zheng H et al. *Science* **303** 661 (2004)
253. Yan L et al. *Appl. Phys. Lett.* **94** 192902 (2009)
254. Yang C-H et al. *Nature Mater.* **8** 485 (2009)
255. Choi T et al. *Science* **324** 63 (2009)
256. Yang S Y et al. *Nature Nanotechnol.* **5** 143 (2010)
257. Seidel J et al. *Phys. Rev. Lett.* **107** 126805 (2011)
258. Kundys B et al. *Nature Mater.* **9** 803 (2010)
259. de Sousa R, Moore J E *Appl. Phys. Lett.* **92** 022514 (2008)
260. Mills D L, Dzyaloshinskii I E *Phys. Rev. B* **78** 184422 (2008)
261. Zvezdin A K, Mukhin A A *Pis'ma Zh. Eksp. Teor. Fiz.* **89** 385 (2009) [*JETP Lett.* **89** 328 (2009)]
262. Rovillain P et al. *Nature Mater.* **9** 975 (2010)
263. Wang L et al. *Sci. Rep.* **2** 223 (2012)
264. Popov Yu F et al. *Ferroelectrics* **204** 269 (1997)
265. Srinivas A, Sritharan T, Boey F Y C *J. Appl. Phys.* **98** 036104 (2005)
266. Matsui T et al. *Appl. Phys. Lett.* **86** 082902 (2005)
267. Belik A A et al. *Angew. Chem. Int. Ed.* **48** 6117 (2009)
268. Kai Chen et al. *Europhys. Lett.* **89** 27004 (2010)
269. Chen X Q et al. *J. Phys. D Appl. Phys.* **43** 065001 (2010)
270. Ashok K et al. *Phys. Status Solidi RRL* **4** (1 – 2) 25 (2010)
271. Zvezdin A K et al. *Zh. Eksp. Teor. Fiz.* **136** 80 (2009) [*JETP* **109** 68 (2009)]
272. O'Dell T H *Philos. Mag.* **16** 487 (1967)
273. Krichevtsov B B, Pavlov V V, Pisarev R V *Pis'ma Zh. Eksp. Teor. Fiz.* **49** 466 (1989) [*JETP Lett.* **49** 535 (1989)]
274. Stefanovskii E P *Ferroelectrics* **161** 245 (1994)
275. Khalfina A A, Shamtsutdinov M A *Ferroelectrics* **279** 19 (2002)
276. Tanygin B *J. Magn. Magn. Mater.* **323** 616 (2011)
277. Shamsutdinov M A, Kharisov A T, Nikolaev Yu E *Fiz. Met. Metalloved.* **111** 472 (2011) [*Phys. Met. Metallogr.* **111** 451 (2011)]
278. Gerasimchuk V S, Shitov A A *Fiz. Tverd. Tela* **54** 79 (2012) [*Phys. Solid State* **54** 84 (2012)]
279. Guslienko K Yu *J. Nanosci. Nanotechnol.* **8** 2745 (2008)
280. Van Waeyenberge B et al. *Nature* **444** 461 (2006)
281. Khvalkovskiy A V et al. *Appl. Phys. Lett.* **96** 212507 (2010)
282. Delaney K T, Mostovoy M, Spaldin N A *Phys. Rev. Lett.* **102** 157203 (2009)
283. Pyatakov A P, Meshkov G A, Logginov A S *Vestn. Mosk. Univ. Ser. 3 Fiz. Astron.* (4) 91 (2010)
284. Shigeto K et al. *Appl. Phys. Lett.* **80** 4190 (2002)
285. Mironov V L et al. *Phys. Rev. B* **81** 094436 (2010)
286. Zvezdin K A *Fiz. Tverd. Tela* **42** 116 (2000) [*Phys. Solid State* **42** 120 (2012)]
287. Meshkov G A et al. *J. Magn. Soc. Jpn.* **36** (1 – 2) 46 (2012)
288. Logginov A S et al. *Pis'ma Zh. Eksp. Teor. Fiz.* **66** 398 (1997) [*JETP Lett.* **66** 426 (1997)]
289. Krotenko E B, Melikhova Yu V, Yablonskii D A *Fiz. Tverd. Tela* **27** 3230 (1985)
290. Logginov A S et al. *J. Magn. Magn. Mater.* **310** 2569 (2007)
291. Tanygin B M *J. Magn. Magn. Mater.* **324** 1659 (2012)
292. Wang Y et al. *Adv. Mater.* **23** 4111 (2011)
293. Zhai J et al. *Appl. Phys. Lett.* **88** 062510 (2006)
294. Dong Sh, Li J-F, Viehland D *Appl. Phys. Lett.* **85** 2307 (2004)
295. Quandt E et al. *Rev. Sci. Instrum.* **78** 106103 (2007)
296. Filippov D A, Galkina T A, Srinivasan G *Pis'ma Zh. Tekh. Fiz.* **36** (21) 23 (2010) [*Tech. Phys. Lett.* **36** 984 (2010)]
297. Filippov D A, Galkina T A, Laletin V M *Inversnyi Magnitoelektricheskii Effekt v Magnitostriktsionno-p'ezoelektricheskikh Strukturakh* (Inverse Magnetoelectric Effect in Magnetopiezoelectric Structures) (Velikii Novgorod: Pechatnyi Dvor 'Velikii Novgorod', 2011)
298. Bush A A et al. *Zh. Tekh. Fiz.* **79** (9) 71 (2009) [*Tech. Phys.* **54** 1314 (2009)]
299. Ghosh A, Sheridon N K, Fischer P *Small* **4** 1956 (2008)
300. Lin T-J et al. *Appl. Phys. Lett.* **93** 013108 (2008)
301. Ghoshal U S, US Patent 6,535,342 (2003)
302. Tiejun Zhou et al. *Appl. Phys. Lett.* **96** 012506 (2010)
303. Parkin S S P, Hayashi M, Thomas L *Science* **320** 190 (2008)
304. Parkin S S P, US Patent 7,031,178 (2006)
305. Vanhaverbeke A, Bischof A, Allensoach R *Phys. Rev. Lett.* **101** 107202 (2008)
306. Hu J-M et al. *J. Appl. Phys.* **108** 043909 (2010)
307. Chung T-K, Carman G P, Mohanchandra K P *Appl. Phys. Lett.* **92** 112509 (2008)
308. Brintlinger T et al. *Nano Lett.* **10** 1219 (2010)
309. Fert A *Rev. Mod. Phys.* **80** 1517 (2008)
310. Binek Ch, Doudin B *J. Phys. Condens. Matter* **17** L39 (2005)
311. Gajek M *Nature Mater.* **6** 296 (2007)

312. Wu S M et al. *Nature Mater*. **9** 756 (2010)
313. Garcia V et al. *Science* **327** 1106 (2010)
314. Stolichnov I et al. *Nature Mater*. **7** 464 (2008)
315. Riester S W E et al. *Appl. Phys. Lett*. **94** 063504 (2009)
316. Wu T et al. *Appl. Phys. Lett*. **98** 262504 (2011)
317. Roy K, Bandyopadhyay A, Atulasimha J *Appl. Phys. Lett*. **99** 063108 (2011)
318. Fashami M S et al. *Nanotechnology* **22** 155201 (2011)
319. Datta S, Das B *Appl. Phys. Lett*. **56** 665 (1990)
320. Jia C, Berakdar J *Appl. Phys. Lett*. **95** 012105 (2009)
321. Kamentsev K E, Fetisov Y K, Srinivasan G *Appl. Phys. Lett*. **89** 142510 (2006)
322. Ma J et al. *J. Magn. Magn. Mater*. **323** 101 (2011)
323. Khitun A, Nikonov D E, Wang K L *J. Appl. Phys*. **106** 123909 (2009)
324. Krichevtsov B B, Pisarev R V, Selitskii A G *Zh. Eksp. Teor. Fiz*. **101** 1056 (1992) [*Sov. Phys. JETP* **74** 565 (1992)]
325. Koronovskyy V E, Ryabchenko S M, Kovalenko V F *Phys. Rev. B* **71** 172402 (2005)
326. Inoue M et al. *J. Appl. Phys*. **83** 6768 (1998)
327. Steel M J, Levy M, Osgood R M (Jr.) *J. Lightwave Technol*. **18** 1297 (2000)
328. Belotelov V I, Zvezdin A K *J. Opt. Soc. Am. B* **22** 286 (2005)
329. Inoue M et al. *J. Phys. D Appl. Phys*. **39** R151 (2006)
330. Sawada K, Nagaosa N *Appl. Phys. Lett*. **87** 042503 (2005)
331. Goto T et al. *J. Appl. Phys*. **109** 07B756 (2011)
332. Da H-X, Huang Z-Q, Li Z Y *Opt. Lett*. **34** 356 (2009)
333. Qiu Ch-W et al. *Phys. Rev. B* **75** 245214 (2007)
334. Kamenetskii E O, Sigalov M, Shavit R *J. Appl. Phys*. **105** 013537 (2009)
335. Kulagin D V et al. *Pis'ma Zh. Eksp. Teor. Fiz*. **92** 563 (2010) [*JETP Lett*. **92** 511 (2010)]
336. Kulagin D V et al. *Zh. Eksp. Teor. Fiz*. **141** 540 (2012) [*JETP* **114** 474 (2012)]
337. Li P et al. *Sensors Actuators A* **157** 100 (2010)
338. Majdoub M S, Sharma P, Çağin T T *Phys. Rev. B* **78** 121407(R) (2008)
339. Dong Sh et al. *Appl. Phys. Lett*. **93** 103511 (2008)
340. Mitcheson P D et al. *Proc. IEEE* **96** 1457 (2008)